Human Neurophysiological Mechanisms of Contextual Modulation in Primary Visual Cortex

A DISSERTATION
SUBMITTED TO THE FACULTY OF THE GRADUATE SCHOOL
OF THE UNIVERSITY OF MINNESOTA
BY

Jennifer Frances Schumacher

IN PARTIAL FULFILLMENT OF THE REQUIREMENTS
FOR THE DEGREE OF
DOCTOR OF PHILOSOPHY

Dr. Cheryl A. Olman, Advisor
Dr. Daniel J. Kersten, Co-Advisor

May 2010

Acknowledgements

I am very thankful for my strong support network during my graduate studies. I am convinced I had the best advisors – Cheryl and Dan, thank you for your guidance I am eternally grateful for the knowledge you have imparted upon me. Thanks also to Steve, Matt, and Guillermo who served as the rest of my committee, I appreciated the suggestions to improve my experiments. I could not have survived this experience without the support of my family – thanks especially to my parents who were always there to listen and interested in my work (Dad, the radar stuff did not make it in… but someday I promise!) A huge thanks to my classmates and labmates – I will cherish our neuronerd memories forever; and to those who got me through the final stretch.

Abstract

This dissertation examines visual processing of contextually modulated artificial and natural stimuli in primary visual cortex on a local scale. Understanding how local features are integrated into a global structure or ignored as irrelevant background is a critical step in comprehending human vision. To investigate these mechanisms, first it was necessary to measure the relationship between inferred neural responses, such as those obtained with blood oxygenation level-dependent (BOLD) fMRI, and local stimuli. From this point, orientation-dependent contextual modulation was analyzed locally or with a contour. While focusing on primary visual cortex, these experiments with stimuli of increasing complexity provide a foundation for how local features are grouped into global structures.

BOLD fMRI provides a non-invasive method to measure the inferred neural response in humans. Because BOLD fMRI is a result of interaction between neural activity, blood flow, and deoxyhemoglobin concentration, it is not obvious that there is a linear relationship between these mechanisms as well as established functions, like the contrast response function (CRF). Chapter 2 measures the BOLD response to single Gabor patches of increasing contrast with two pulse sequences: Gradient Echo (GE) and Spin Echo (SE). GE measurements include signals from large and small veins while SE measurements eliminate the signal from large veins. Comparing these signals, at ultra-high field strength (7 Tesla) found the relationship between the CRF and BOLD fMRI for local stimuli is not linear with GE measurements.

Chapters 3 and 4 focus on orientation-dependent contextual modulation of a single Gabor patch or of a vertical line of Gabor patches. In the periphery, surrounds of parallel orientation suppress the center stimulus while surrounds of orthogonal orientation facilitate the center stimulus. The relationship between the BOLD response and these suppressive or facilitative mechanisms was measured on a local scale (Chapter 3). Then, to compare the mechanisms for orientation-dependent contextual modulation and contour

integration, performance in a contour detection task was measured over an extensive parameter space (Chapter 4). These data show that the BOLD response to suppressive stimuli do not behave as predicted by psychophysical results and that orientation-dependent contextual modulation and contour integration operate over different spatial scales, and likely different neural mechanisms.

This dissertation provides data on the relationship between the BOLD response and local stimuli as well as data on the neural mechanisms behind orientation-dependent contextual modulation, contour integration, and texture classification. An over-arching theme is that inferred neural responses, such as those measured with BOLD fMRI, behave differently on a local scale than a global scale. However, other non-invasive measures provide details for how local stimuli are processed and further integrated into a global structure. Future work can incorporate computational models of neural activity and the BOLD response to clarify why measured responses differ on a local scale compared to a global scale.

Table of Contents

Acknowledgements i

Abstract ii

Table of Contents iv

List of Tables v

List of Figures vi

Chapter 1 Early Visual Processing: Contextual Modulation and Methods 1

Chapter 2 Contrast Response Functions for Single Gabor Patches: GE BOLD Over-Represents Low-Contrast Patches but SE BOLD Does Not 7

Chapter 3 High-Resolution BOLD fMRI Measurements of Local Orientation-Dependent Contextual Modulation Show a Mismatch between Predicted V1 Output and Local BOLD Response 27

Chapter 4 Collinear Facilitation and Orientation-Dependent Inhibitory Mechanisms Operate on Different Spatial Scales in a ContourDetection Task 57

Bibliography 70

List of Tables

Table 1: Fit parameters for threshold vs. contrast functions 11

Table 2: Parameter values implemented to fit the TvC curves. 33

List of Figures

Figure 1.1: Adelson Illusion. 2
Figure 1.2: Natural image of horse.. 3
Figure 1.3: Schematic of the BOLD response. 5
Figure 2.1: Stimuli used to study the BOLD fMRI contrast response in V1. 12
Figure 2.2: Gradient Echo (GE) BOLD and Spin Echo (SE) BOLD hemodynamic responses. ... 18
Figure 2.3: Contrast response functions for GE and SE BOLD.. 20
Figure 2.4: Contrast response functions for large patches of sinusoidal gratings……...18
Figure 3.1: Stimuli used to study contextual modulation in V1.. 30
Figure 3.2: Psychophysical quantification of suppression of target Gabor responses 41
Figure 3.3: ROI localization. 43
Figure 3.4: Estimated BOLD fMRI responses in target ROI.. 45
Figure 3.5: Discrimination thresholds for parallel flankers 46
Figure 3.6: BOLD response to target-alone Gabor patches. 47
Figure 3.7: Annulus experiment results. 48
Figure 4.1: Examples of stimuli with collinear Gabors present on the left side.. 62
Figure 4.2: Example of a psychometric function. 63
Figure 4.3: Control condition results.. 64
Figure 4.4: Orthogonal context results..... 66
Figure 4.5: Performance on control and parallel condition relative to orthogonal condition.. 67

Chapter 1

Early Visual Processing: Contextual Modulation and Methods

Human vision is a sensory system that has yet to be replicated – computer vision is still far from efficiently and effectively identifying objects in natural scenes. Vision research has a wealth of background material, from Hecht, Schler, and Prin's studies on photons (1942) to Hubel and Weisel's classic work on orientation columns (1959) to modern functional imaging that can predict what image a subject is viewing (Kamitani & Tong 2005; Kay, Naselaris et al. 2008). However, there are still gaps in the current literature regarding contextual modulation in early visual cortex, particularly on a local scale.

Understanding neural circuitry on a local scale is important because much of the past work has been performed on a single neuron level (and thereby not capturing the neural population code) or by averaging over a large piece of cortex (and thereby averaging over local network responses, such as responses features of a visual scene). It is not clear that single neuron responses are even strongly correlated with population activity (Scannell & Young, 1999). Therefore, it is important, and the focus of this dissertation, to measure and quantify neural responses on a local level, to individual features in a visual scene with contextual modulation.

Contextual Modulation

A classic example of contextual modulation is the Adelson illusion (Figure 1.1), where squares A and B appear to be of different luminance, however it is just the context of the cylinder's shadow and the checkerboard pattern that make these identical squares

appear different. Thus, this illusion emphasizes that the local context of features in a visual scene is critical to global perception and the associated neural activity. Measurement of the local neural responses to square A and B with and without the context of the rest of the visual scene could reveal further insight into how early visual areas process local features into a global percept.

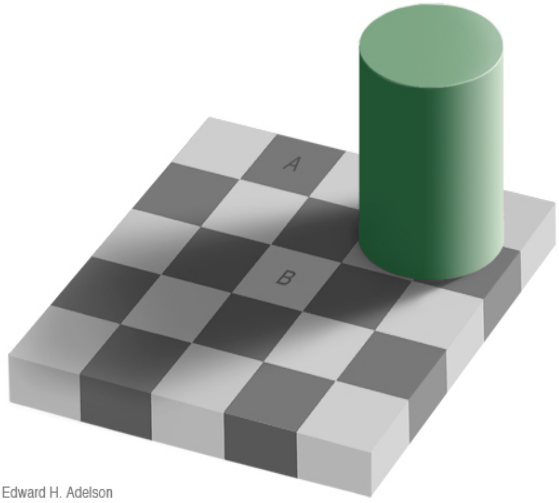

Figure 1.1: Adelson Illusion. Contextual modulation of local features makes squares A and B appear to be of different luminance values; however they are actually the same value. {http://web.mit.edu/persci/people/adelson/checkershadow_illusion.html}

Contextual modulation is also critical in the natural world. It is also allows one to investigate the same population of neurons as it is modulated by a different percept – often requiring completely different neuronal mechanisms. It is important to understand how individual features of a scene are grouped together into an object, or ignored as irrelevant background. For example in Figure 1.2, a natural scene of a horse in a meadow, where the fence post occludes the horse's front leg. Cues such as texture help the visual observer group the fence posts together and the horse legs together and realize that the fence post is not a horse leg, and that the horse does not only have three legs. It is likely contextual modulation mechanisms develop both from intra-cortical connections and feedback connections from higher visual areas (Zipser, Lamme et al. 1996; Crist, Li et al. 2001)

Figure 1.2: Natural image of horse. Occlusion of one of the horse's front legs by the fence post makes cues such as texture important for grouping features of the scene into objects (horse parts and fence posts in this case).

Surround Suppression

Surround suppression is one type of contextual modulation that plays a central role to sensation and perception and involves one population of neurons suppressing the response from another population of neurons. Neural inhibition, the mechanism believed to influence surround suppression, is a fundamental aspect of visual processing, playing a role in neural computations both between and within cortical areas of the brain. It is thought to be critical to vision, as it plays a role in parsing visual scenes into figures and background, such as at texture boundaries (Grigorescu, Petkov et al., 2004). However inhibitory mechanisms are difficult to study because of the small size and low density of inhibitory neurons in the cerebral cortex; as the relative density of inhibitory neurons in the cortex is 14-17% (Patel, de Graaf et al. 2005). Therefore, for the purposes of this dissertation, it will be assumed that surround suppressive mechanisms could also include subcortical activity via feedback from V1 to the lateral geniculate nucleus or feedback connections from V2 in addition to connections within V1 (Knierim & van Essen, 1992).

Methods

In order to analyze contextual modulation on a local scale, it is necessary to use methods that will reveal a multi-dimensional representation of a single chunk of cortex. Psychophysics and high-resolution BOLD fMRI provide measurements of inferred neural responses that allow measurements of local neurophysiological mechanisms of context-driven activity. Psychophysical experiments associate behavioral results with correlations to inferred neural activity measurements by using stimuli tuned to specific properties of sensory cortex. BOLD fMRI corresponds activity in individual voxels during functional imaging where changes in the concentration of deoxyhemoglobin are associated with increases in neural activity.

Psychophysics

Detection thresholds are linked to neural activity in primary visual cortex where neural responses encode information needed to make a perceptual decision. Measurements of human behavior in response to small changes in the properties of physical stimuli give insight to the neural mechanisms controlling these behavioral decisions. In the case of surround suppression, good correspondence between psychophysics and electrophysiological results has been found (Knierim and van Essen 1992; Zenger-Landolt and Koch 2001). Therefore it is appropriate to use non-invasive means to study surround suppression in humans to investigate the underlying neural mechanisms.

BOLD fMRI

Blood oxygenation level-dependent (BOLD) functional magnetic resonance imaging (fMRI) measures inferred neural responses by associating a decrease in deoxyhemoglobin concentration with an increase in image contrast (Figure 1.3). The BOLD response arises after neural activity, which increases blood flow as well was increases the oxygenation extraction fraction. This causes the concentration of deoxyhemoglobin in the veins near this neural activity to decrease which gives rise to an increase in the BOLD response. The subsequent hemodynamic response peaks after about

6 seconds, is typically around 1% change from baseline with gradient echo pulse sequences, and returns to baseline after 15 seconds.

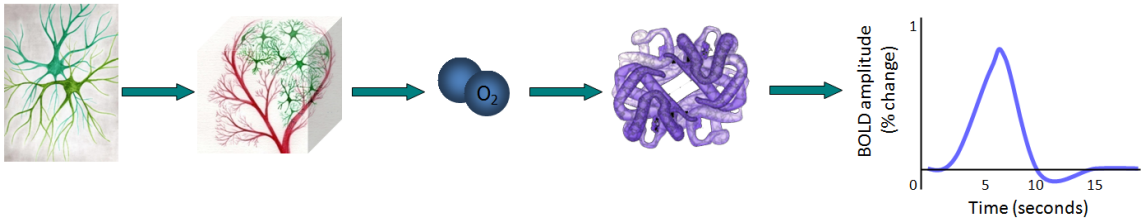

Figure 1.3: Schematic of the BOLD response.

BOLD fMRI & Neural Inhibition

The BOLD fMRI response to local lateral inhibition is not thoroughly understood; and the field is divided about whether there will be an increase or decrease in BOLD response to neural inhibition. In the cerebellum, it was found that the hemodynamic response can increase even when spiking is inhibited (Lauritzen, 2001). GABAergic neurons (where GABA is an inhibitory neurotransmitter) have the ability to constrict or dilate microvessels when stimulated, thereby making them capable changing the hemodynamic response in either direction (Cauli, et al. 2004). Nie & Wong-Riley colocalized GABAergic neurons with cytochrome oxidase, an indicator of metabolic demand, suggesting that inhibitory neurons require more energy than excitatory neurons (1995). Local field potentials have been slightly better correlated with the BOLD response compared to spiking rates (Logothetis, et al., 2004). On the other hand, there is also a large support for observing a decrease in BOLD response to local neural inhibition (Zenger-Landolt & Heeger, 2003). In general, it has been maintained that the BOLD response is proportional to metabolic activity, which is proportional to synaptic activity and thereby average firing rates, thus making the assumption that a decrease in firing rate would result in a decrease in BOLD response (Heeger, et al., 2000). However, it is not clear what metabolic demand inhibitory neurons have – either negligible or significant (Patel, et al., 2005; Ackermann, et al., 1984; Sotero & Trujillo-Barreto, 2007). Negative BOLD responses have also been associated with inhibitory activity (Stefanovic, Warnking et al. 2004; Shmuel, Augath et al. 2006). Finally, it has been shown that increased levels of endogenous GABA results in a decreased hemodynamic response

(Chen, et al. 2005). A wide range of methodologies, from in vitro to in vivo, have supported observing both increases and decreases in BOLD response to local neural inhibition.

Significance

It is apparent that contextual modulation, and specifically surround suppression, is an important feature of visual processing. More generally, a loss of inhibitory function, such as in Parkinson's patients (Anderson, et al., 2006), could also benefit from a great understanding of feedback mechanisms, and specifically the role of inhibition. There is also evidence that schizophrenics fail at perceiving contextual modulation (Silverstein, et al., 2000; Ulhaas, et al., 2004; Dakin, et al., 2005). Understanding the functional changes of the neural mechanisms underlying the cortical damage observed in traumatic brain injuries and other neurological disorders will provide opportunities to develop rehabilitation techniques for these patients. One possible treatment, cortical implants, could be further developed to replace the malfunctioning neural connections in either of these cases. Additionally, computational models provide a foundation for understanding the neural mechanisms behind early visual processing, but further data are needed to constrain assumptions about the role of inhibition in contextual modulation. Processed images from the model could supplement human observers' ability in identifying targets, such as finding abnormalities in radiology images. Therefore, developing a model mimicking human neurophysiological responses will provide information for developing new methodologies to assist visual discrimination and detection tasks. The systems-level approach used here provides some information necessary for the design of new treatments and improvement of computational models.

Chapter 2

Contrast Response Functions for Single Gabor Patches: GE BOLD Over-Represents Low-Contrast Patches but SE BOLD Does Not

Authors: Jennifer F. Schumacher, Serena K. Thompson, Cheryl A. Olman

To be submitted to *Journal of Vision*

Abstract

Crucial for the interpretation of BOLD fMRI data is a linear relationship between the BOLD response and underlying neural activity. This relationship has been tested many times in early visual cortex and found to be linear. These studies have used stimuli that subtend a large visual angle or fill the entire visual field to test the BOLD response; however, the present study tests whether the BOLD response is linearly related to the underlying neural activity when only a small patch of cortex is stimulated. The BOLD response to isolated Gabor patches was measured with gradient echo (GE) BOLD and spin echo (SE) BOLD at 7 Tesla. Our primary finding is an excessively large GE BOLD response to low-contrast, isolated Gabor patches, such that the BOLD contrast response function is not monotonically related to the underlying neural contrast response. In addition, we find that the event-related SE BOLD response does not show the same amplification of low-contrast responses. A control experiment with larger sinusoidal gratings measured both SE and GE BOLD responses that were linearly related to inferred neural activity, even for low contrasts. These experiments therefore confirm the linearity of the relationship between BOLD activity and underlying neural activity for large stimuli, but not for low-contrast, small image features.

Introduction

The value of BOLD fMRI as a non-invasive indicator of neural activity in the human brain is greatest if the BOLD response is linearly related to the underlying neural activity. Many studies have investigated the linearity of the relationship between BOLD signal changes and measured or inferred neural activity, finding in general that neurohemodynamic coupling behaves, by and large, as a linear system (Boynton, Engel et al. 1996; Boynton, Demb et al. 1999; Logothetis, Pauls et al. 2001; Heckman, Bouvier et al. 2007; Zhang, Zhu et al. 2008).

Because previous studies have generally used full-field or extended visual stimuli, which stimulate large regions of cortex, the present study was designed to test the linearity of the BOLD response to small visual stimuli, which produce well-localized patches of neural activity (approximately 5 mm in diameter) in early visual cortex. These relatively weak stimuli could potentially unveil nonlinear aspects of the hemodynamic response, such as local oxygen consumption without concomitant increases in local blood flow (resulting in a BOLD signal lower than predicted for low-contrast stimuli), or an over-exuberant BOLD signal at low contrast due to a lack of fine resolution in local blood flow recruitment. We therefore used standard gradient echo (GE) BOLD as well as spin echo (SE) BOLD to study, in different vascular compartments, the linearity of the BOLD response to isolated Gabor patches at a range of luminance contrasts.

As an alternative to the more common GE BOLD techniques that use T_2*-weighted images to maximize sensitivity to magnetic field perturbations in and near veins (Ogawa, Menon et al. 1993; Bandettini, Wong et al. 1994), SE BOLD techniques use T_2-weighted images to bias BOLD sensitivity toward small venuoles and capillaries (Norris, Zysset et al. 2002; Duong, Yacoub et al. 2003; Yacoub, Duong et al. 2003; Hulvershorn, Bloy et al. 2005; Parkes, Schwarzbach et al. 2005). At low field strengths, SE BOLD is also sensitive to intravascular blood contributions in large veins (Oja, Gillen et al. 1999), but at high field strength (e.g., 7 Tesla), the short T_2 of venous blood removes this residual contribution from large veins (Duong, Yacoub et al. 2003). We were therefore interested in testing the linearity of both GE BOLD and SE BOLD techniques at 7T, to discover whether nonlinearities in the BOLD response are more likely attributable to large-diameter or small-diameter vascular compartments. While we observed

a linear SE BOLD response across all stimulus conditions, we found that the GE BOLD response to isolated, 5% contrast Gabor elements was inordinately high.

Methods

Subjects

The psychophysics and fMRI data were collected from six human subjects (five female, age 25 – 35) with normal or corrected to normal vision. Subjects participated in one or both of the experiments described below after providing written informed consent. The experimental protocols conformed to safety guidelines for MRI research and were approved by the Institutional Review Board at the University of Minnesota.

Visual Stimuli

The visual stimulus (Figure 2.1A) consisted of four Gabor patches located in each of the four visual quadrants at three degrees eccentricity. Each Gabor patch consisted of a 3 cycles-per-degree (cpd) sinusoidal grating modulated by a Gaussian envelope with full width at half-maximum of 0.6 degrees (σ = 0.25 degrees). All stimuli were presented on a mean gray background. Stimuli were generated and presented with Matlab (Mathworks, Inc., Natick, MA) and Psychtoolbox (Brainard, 1997). Macintosh iMac computers with OS X served as the processors for the psychophysics and fMRI system. For psychophysical measurements of contrast discrimination thresholds, stimuli were displayed on an NEC 2180UX LCD monitor, subtending 8 x 11 degrees of visual angle at a viewing distance of 200 cm. For the 7T experiments, stimuli were projected onto a screen behind the subjects' heads (Sanyo projector with custom lens made by Navitar), which was viewed via a mirror mounted on the head coil. Total image area subtended 12 x 16 degrees at a viewing distance of 71 cm.

For the control experiment, larger patches of 3 cpd sinusoidal gratings replaced the Gabors. The patches were centered at 3 degrees eccentricity and had a radius of 2 degrees. The patches were defined by a circular mask with hard edges.

Psychophysics

Contrast response functions for target Gabors were estimated from contrast discrimination thresholds. For these psychophysical measurements, a Bits^{++} digital video processor (Cambridge Research Systems Ltd., UK) was used to provide 14-bit brightness resolution. Eight pedestal contrasts were employed for the target Gabor patches: 0%, 1%, 2%, 4%, 8%, 16%, 32%, and 64%. On each trial, all four targets appeared. On one of the two intervals in the trial, one of the four targets was incremented in contrast. The stimulus was presented for 250 ms in each interval, with a 500 ms blank inter-stimulus interval. Subjects maintained fixation on a white square at the center of the stimulus set while indicating the interval (1 or 2) in which one of the target Gabors increased in contrast; feedback for the task was given by a green ('correct') or red ('incorrect') color at fixation after each response. A 3-down 1-up staircase was used to control the contrast increment on each trial; this staircase converged at a performance level of 79% correct, which was used as the threshold estimate for each pedestal contrast for each stimulus condition. Five threshold estimates (3-5 runs of 40 trials) at each of the eight contrast levels were completed per subject.

Threshold versus contrast (TvC) curves for each condition and each stimulus type were fit (using Matlab's lsqcurvefit function) with the Naka-Ruston formula (Equation 1.1). The inferred contrast-response function for each stimulus configuration is the integral of this function. Parameters used to fit the data for each subject are shown in Table 1 and an example TvC curve and CRF are shown in Figure 1C.

Equation 2.1: $r(x) = ac^{p+q} / (c^q + \sigma^q)$

Table 2.1: **Fit parameters for threshold vs. contrast functions**

Subject	a	p	q	σ
1	68.5601	1.3232	-0.8693	2.6467
2	53.8414	1.1399	-0.9195	11.1685
3	55.4740	1.2585	-1.1088	7.3510
4	56.9999	1.3795	-0.9373	2.484
5	62.5446	1.3625	-0.8875	1.6681
6	56.9427	1.3416	-0.9128	2.3320

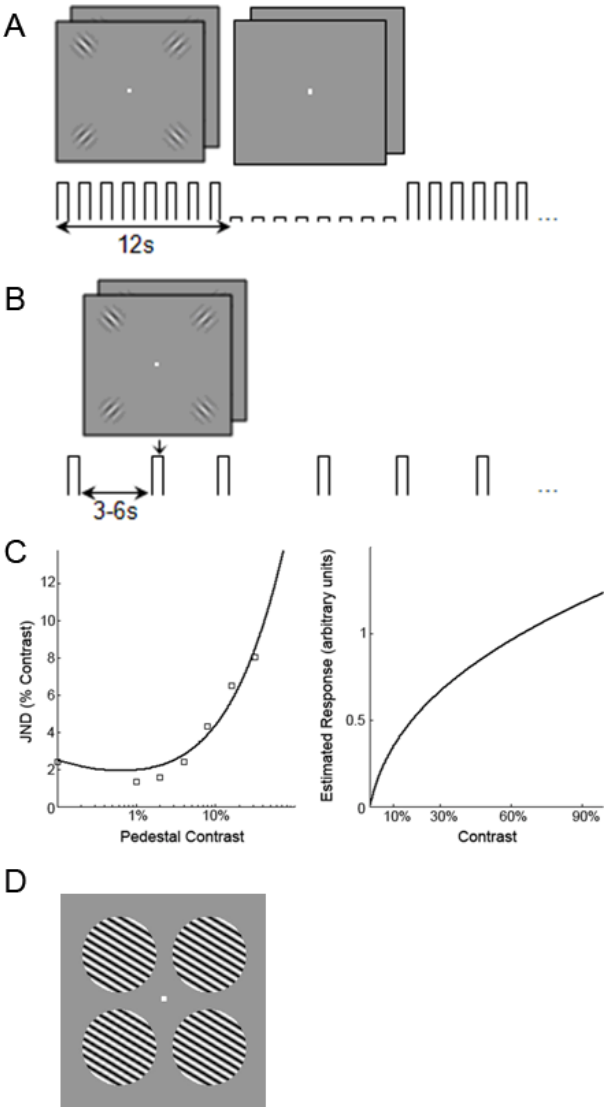

Figure 2.1: Stimuli used to study the BOLD fMRI contrast response in V1. (A) Block-design localizer scans were used to select regions of interest for analysis of the event-related data. Subjects were engaged in the same 2AFC task during localizer scans. During "on" blocks stimuli were presented at 80% pedestal contrast (8 trials per 12-second block); during "off" blocks pedestal contrast was 0%. (B) Stimuli for event related scans were presented at 5%, 10%, 30% and 90% contrast with inter-stimulus intervals randomly distributed between 3-6 seconds. Stimuli were presented as a 2-interval forced choice paradigm; subjects were required to detect a contrast increment on one of the four Gabor elements in one of the two intervals; a 3-down 1-up staircase adjusted the contrast increment to equate difficulty between the four contrast conditions. (C) Psychophyiscal measurements of contrast increment threshold (left column) were used to infer the V1 contrast response function (right column) for each subject.

MRI Systems

The 7 Tesla magnet (Magnex Scientific, UK) was equipped with a Siemens console (Erlangen, Germany) and a Siemens Avanto head gradient set capable of 80 mT/m and a maximum slew rate of 333 T/m/s. A half volume coil was used for RF transmission and a small (6 cm) quadrature coil was used for reception (Adriany, Pfeuffer et al. 2001); these coils were actively detuned during the acquisition.

fMRI Experiments

Main experiment: Event-related GE and SE BOLD responses at 7T to isolated Gabor patches. All data for individual subjects were acquired in a single scanning session that contained four types of scans: GE BOLD block-design localizers, SE BOLD block-design localizers, GE BOLD event-related runs, and SE BOLD event-related runs. Regions of interest were defined by block-design localizer scans, during which subjects were engaged in a 2IFC contrast-discrimination task. Behavioral responses were collected using a fiber-optic button box (Current Designs, Philadelphia, PA). Stimulus durations and inter-stimulus/inter-trial intervals were shorter during localizers than during psychophysical and event-related measurements: stimulus duration was 150 ms stimulus separated by a 100 ms inter-stimulus interval, with trials (paired stimulus presentation) occurring every 1.5 s (8 trials per block). “On” and “off” blocks each lasted 12 seconds; 11 “on” blocks alternated with 10 “off” blocks during each scan, and the first half-cycle (“on”) block was discarded before analysis. During “on” blocks the pedestal contrast was 80%; during “off” blocks the target pedestal contrast was 0%. Two or three GE localizer scans and two or three SE localizer scans were included in each experiment, depending on the stamina of the subject.

The event-related scans measured BOLD response to four stimulus conditions (target contrasts): 5%, 10%, 30% and 90% Michelson contrast. Stimuli were presented in the same 2IFC contrast-discrimination task as in the psychophysics, with an inter-trial interval of 3, 4.5 or 6 seconds (inter-trial interval was randomly selected and uniformly

distributed). There were a total of 48 trials per scan, 12 at each contrast level, for a total of 60-96 presentations of each contrast level for each subject for each BOLD technique (5-8 GE BOLD event-related scans and 5-8 SE BOLD event-related scans per subject).

EPI data were acquired at a rate of one volume every 1.5 s. Field of view was 128 mm x 96 mm with a matrix size of 64 x 48 (6/8 partial Fourier) for a nominal in-plane resolution of 2 mm isotropic. Slice thickness was 2 mm, volume repetition time (TR) was 1.5 seconds, and 12 slices were prescribed perpendicular to the calcarine sulcus in an oblique coronal orientation to cover primary visual cortex. For the GE BOLD data echo-spacing was 0.41 ms (read-out time for one line) and echo time (TE) was 20 ms; for the SE BOLD data echo-spacing was 0.41 ms and TE was 50 ms.

Control experiment: Event-related GE and SE BOLD responses at 7T to large sinusoidal grating patches. The experiment design was identical to the main experiment except the Gabor patches were replaced by larger patches of sinusoidal gratings subtending 4 degrees of visual angle. Experiment design and EPI data acquisition were identical (GE and SE BOLD block-design localizers and event-related scans).

fMRI Data Analysis: pre-processing and localizers

Preprocessing of functional data, which included motion compensation, high-pass filtering and alignment of functional data to the reference anatomy (Nestares and Heeger 2000) was accomplished with custom Matlab code. GE EPI and SE EPI functional runs were acquired in an interleaved manner throughout the scanning session and were co-registered via motion compensation (with the exception of one subject who completed separate GE BOLD and SE BOLD scanning sessions for the main experiment; data were co-registered and analyzed as the other sets, noting that spatial accuracy is likely worse for this one subject). After motion compensation, but before high-pass filtering, fieldmap-based distortion compensation for the EPI images was completed with FSL (Smith, Jenkinson et al. 2004).

Prior to participating in the fMRI experiments each subject had participated in a separate retinotopic mapping session, which included acquisition of an MP-RAGE anatomy (1 mm isotropic resolution) for anatomical reference and cortical surface definition. For the reference anatomy gray/white matter segmentation, cortical surface reconstruction, and surface inflation and flattening were completed in SurfRelax (Larsson 2001). Standard retinotopic mapping (Sereno, Dale et al. 1995; DeYoe, Carman et al. 1996; Engel, Glover et al. 1997) using rotating wedges and expanding rings was used to identify V1 and an iso-eccentricity band centered at three degrees of visual angle from the fovea. Boundaries for visual areas were translated to the reference anatomy, and from there to the functional data, to restrict where regions of interest (ROIs) would be defined for further analysis.

For each scanning session, ROIs were selected based on retinotopic location and functional localizers. Repetitions of the GE block localizers were averaged together to define GE regions of interest, and repetitions of SE localizers were averaged to define SE ROIs. Voxels with coherence (unsigned correlation with a sinusoid at the block-alternation frequency (Bandettini, Jesmanowicz et al. 1993; Engel, Glover et al. 1997)) exceeding 0.30 in the averaged localizer scans were selected to create the ROIs. This threshold value of coherence > 0.30 would correspond to a significance threshold of $p < 2x10^{-4}$, uncorrected, if noise in the BOLD data were uncorrelated. Permutation analysis on this particular dataset indicates that this coherence threshold was, on average, associated with a median (across subjects) single-voxel uncorrected significance of $p < 4x10^{-4}$ for both the GE BOLD and the SE BOLD data.

ROIs were initially defined on a flattened cortical representation, where V1 and eccentricity boundaries could be used to identify the appropriate clusters of voxels. Selected voxels were translated to the inplane anatomy for further refinement to comprise four clusters of contiguous voxels corresponding to the four stimuli in the four visual quadrants. Expected volume of activation was calculated from the average cortical

magnification functions in humans reported in (Engel, Glover et al. 1997), using 2σ and 3σ cut-off points to estimate the diameter of the cortical representation of the Gabor patch and 3 mm as the estimate of the average local cortical gray matter thickness.

fMRI Data Analysis: event-related data analysis

A generalized linear model (GLM) was used to estimate the hemodynamic responses to the stimuli in the event-related design. Custom Matlab code estimated the amplitude of the BOLD response for twelve timepoints (18 s) after the stimulus onset to avoid making assumptions about the shape of the hemodynamic response function (HRF).

Because the scanning sessions were long, the subjects' alertness varied throughout the long scanning sessions. Trials on which subjects failed to respond to the stimuli were therefore excluded from analysis. After selecting only valid trials, the data from separate event-related scans, and the corresponding design matrices, were concatenated and a single HRF estimate was calculated for each ROI in each subject in each 7T scanning session.

Hemodynamic response estimates were fit by a difference-of-gamma (DOG) functions HRF model using the lsqnonlin function in Matlab. Estimated HRFs not adequately fit by the DOG model were excluded from further analysis using the following criteria: peak response within 10s of stimulus onset, full width at half-maximum (FWHM) greater than 0.5 s and less than 6 s, and average error (difference between data and fit) less than the amplitude of the fit.

Results

In our first experiment, we measured the GE and SE BOLD contrast response functions for isolated Gabor patches. First, GE BOLD and SE BOLD block-design localizers were used to define two sets of ROIs (Figure 2.2A). Each set of ROIs in each

subject consisted of four sub-ROIs, corresponding to the four cortical locations of the four Gabor patches. As would be expected either from the lower contrast-to-noise ratio of the SE BOLD technique or from the decreased blurring due to dominance of the small-diameter vascular compartment, the SE BOLD-derived ROIs were smaller than the GE-BOLD derived ROIs. The average volume of a SE BOLD sub-ROI was 115 ± 11 mm^3 (mean ± S.E.M., 28 sub-ROIs); the average volume of a GE BOLD sub-ROI was 276 ± 22 mm^3. Assuming a cortical thickness of 3 mm, and a cortical representation for each Gabor patch approximately 5-8 mm in diameters, the predicted stimulated cortical volume in each location is approximately 75-192 mm^3.

Next, we estimated GE BOLD and SE BOLD event-related hemodynamic response functions (HRFs) for Gabor patches presented at 5%, 10%, 30% and 90% luminance contrast. Estimated HRFs for the SE and GE BOLD response in the SE and GE BOLD-defined ROIs in one representative cortical location from one subject are shown in Figure 2.2B. The primary analyses of interest are the GE BOLD response in the GE BOLD-defined ROIs (upper right panel) and the SE BOLD response in the SE BOLD-defined ROIs (lower left panel). However, the crossed analyses (GE BOLD response in voxels selected by SE BOLD localizer, and *vice versa*, shaded gray in Figure 2.2B) were also performed. Both the GE BOLD and the SE BOLD HRFs are larger in the SE BOLD-derived ROIs (right column).

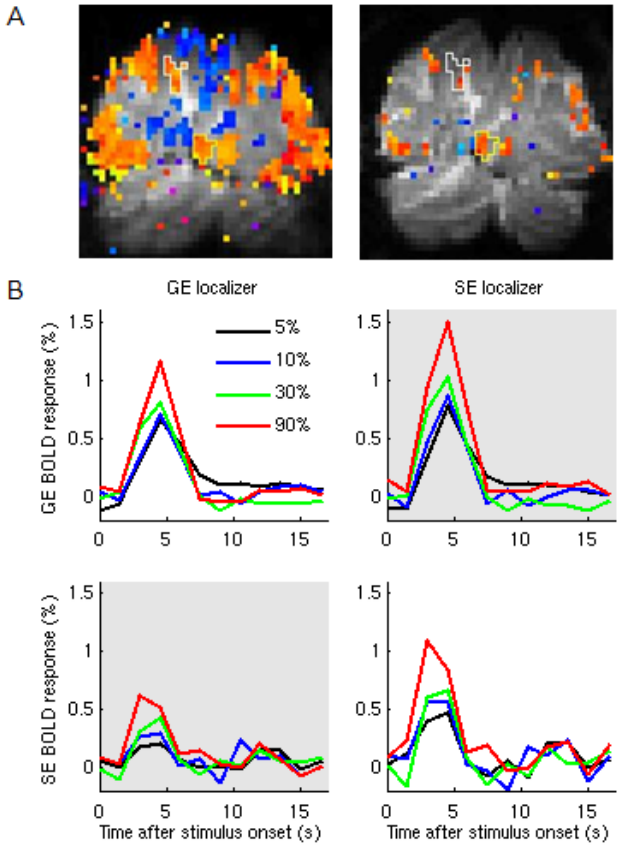

Figure 2.2: Gradient Echo (GE) BOLD and Spin Echo (SE) BOLD hemodynamic responses to Gabor elements of increasing contrast. (A) Voxels for which stimulus coherence exceeded 0.30 in the average of 2 or 3 localizer scans visualized as color overlays on the gray-scale EPI image for a single pseudo-coronal slice. GE data are on the left, SE data are on the right. (B) Estimated hemodynamic responses for voxels selected by the GE BOLD localizer (left column) and the SE BOLD localizer (right column) to Gabor patches of increasing contrast, measured with GE BOLD (top row) and SE BOLD (bottom row).

A single response amplitude was estimated for each contrast in each subject, by combining data from the four subROIs (four cortical locations representing the four Gabor patches) before fitting a difference-of-gamma-functions model to estimate HRF in the combined ROI. Individual estimated HRFs at individual contrasts that were not adequately fit (see Methods for criteria) were excluded from further analysis. BOLD contrast response functions are shown in Figure 2.3A. Because the underlying V1 neural response saturates with increasing contrast, a linear increase in amplitude with increasing

contrast is not expected. However, a monotonic increase is expected and was observed only for the SE BOLD data. Paired t-tests comparing the BOLD response at 5% and 10% amplitude indicate a trend toward the BOLD response to 5% contrast being larger than the BOLD response to 10% contrast (t_5=2.41, p = 0.0604), while the SE BOLD response to 5% contrast was significantly higher than the GE BOLD response to 5% contrast (t_5=-2.58, p = 0.0496).

A linear fit to the BOLD responses, plotted against neural responses estimated from psychophysical measurements (Figure 2.3B), estimates the BOLD response to 0% contrast or the absence of stimulus. BOLD responses to 5% contrast Gabors were excluded from the fits. The linear fit predicts a GE BOLD response of 0.2% for zero-contrast stimuli (black dashed line), and a SE BOLD response of 0.4% (red dashed line), but the 95% confidence for both regressions includes zero.

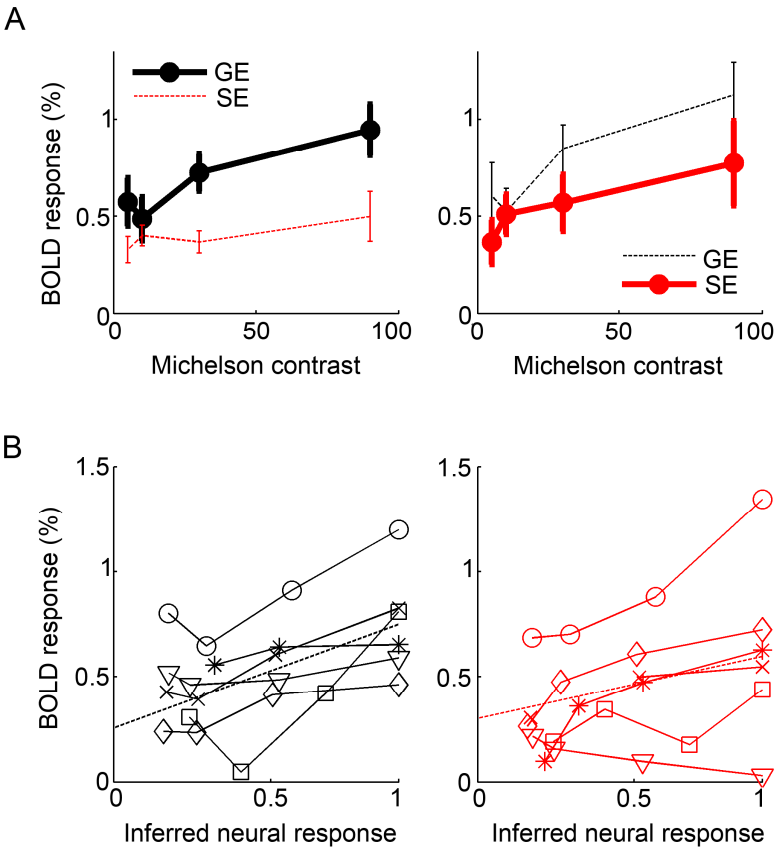

Figure 2.3: Contrast response functions for GE and SE BOLD. A) For each type of ROI (voxels selected by separate GE localizers on left, voxels selected by SE localizer on right), the event-related GE and SE BOLD responses to isolated Gabor patches presented at 5%, 10%, 30% and 90% contrast were estimated for 7 and 6 subjects, respectively (low CNR in one SE dataset precluded analysis). B) BOLD responses for individual ROIs in individual subjects (each subject plotted with a different symbol), plotted against normalized estimates of neural response magnitude, derived from contrast discrimination thresholds. Dashed lines indicate a linear regression to all data. GE BOLD data in GE BOLD ROIs on left; SE BOLD data in SE BOLD ROIs on right.

In a control experiment, we tested whether the apparent non-linearity of the GE BOLD response was a consequence of the small image size or of the rapid event-related experiment design. With an experiment design and analysis identical to the previous experiment, we measured the BOLD response to larger patches of sinusoidal gratings (2° radius) centered at the same eccentricity (3°) in each of the 4 visual quadrants, for four of

the six subjects who participated in the first experiment. As shown in Figure 2.4, the GE BOLD response at 5% contrast was significantly smaller than the response at 10% (t_3=-6.73, p = 0.0067). As in the control experiment, the SE BOLD response at 5% contrast was lower than the response to 10% contrast, but poor fits for the weak SE BOLD response to 5% contrast kept these data from being significant. Regression analysis of the BOLD data with estimated neural responses predicted y-intercepts even closer to zero than in the main experiment (Figure 2.4B).

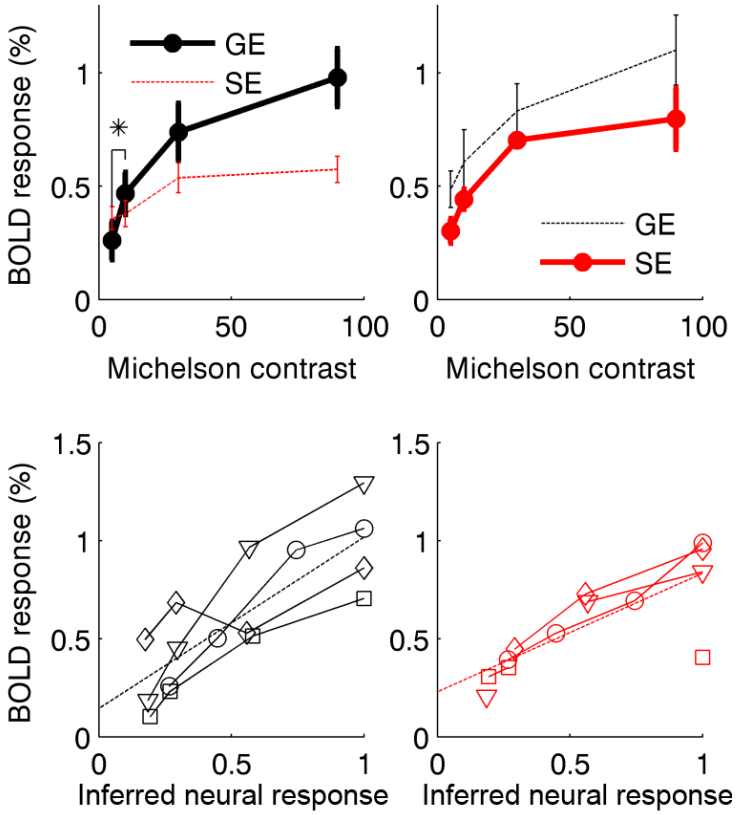

Figure 2.4: GE and SE BOLD contrast response functions for large patches of sinusoidal gratings. A) For each type of ROI (voxels selected by GE localizers on left, voxels selected by SE localizer on right), the event-related GE and SE BOLD responses to extended sinusoidal grating patches presented at 5%, 10%, 30% and 90% contrast were estimated for 4 and 3 subjects, respectively (low CNR precluded analysis of one of the SE datasets). B) Regression between estimates of neural response magnitude, derived from contrast discrimination thresholds, as in Figure 2.3.

Discussion

Our main finding is that the GE BOLD response to small image patches presented at 10% luminance contrast is not significantly larger than the response to patches presented at 5% image contrast, even though the V1 response to 10% contrast Gabors is larger than the V1 response to 5% contrast Gabors. This is not due to a limitation in the contrast-to-noise ratio (CNR) of the experiment because responses to identical stimuli measured with SE BOLD, which has lower CNR, showed a response to 10% contrast patterns that was near significantly larger than the response to 5% contrast patterns. Nor is the overly large response to 5% contrast patterns an artifact of the experiment design, because the GE BOLD response to extended sinusoidal grating patches presented at 10% contrast is significantly larger than the response to 5% contrast gratings. Therefore this non-linearity in the GE BOLD response is apparently limited to low-contrast, small stimuli that elicit spatially restricted patches of relatively weak neural activity on the cortex.

The SE BOLD signal, which contains minimal contributions from large blood vessels, does not show the same lack of linearity that the GE BOLD response shows, which suggests that the overly exuberant BOLD response to low-contrast, isolated Gabor patches may be limited to the large-diameter veins. One possibility to consider is that perfusion may be poorly targeted for isolated, low-contrast stimuli, even though for high-contrast, extended visual stimuli there has been ample demonstration that arterial blood supply as well as the GE BOLD and SE BOLD responses are regulated on a scale much finer than required for the present experiment (Cheng, Wagooner et al. 2001; Duong, Kim et al. 2001; Yacoub, Harel et al. 2008). However, these aforementioned studies have been performed with a differential, block-design protocol, which minimizes the contribution of large veins and therefore studied only perturbations of the blood supply from a high-response state. Poorly targeted perfusion in response to brief (event-related) presentation of isolated, low-contrast stimuli would result in a large positive BOLD

response in cortical territory outside the stimulus representation because increased blood flow in this larger territory would not be mitigated by locally increased oxygen consumption. Only in the center of the territory would the BOLD response reflect a balance of perfusion and oxygen consumption. Larger veins, reflecting changes in deoxyhemoglobin concentrations in both stimulated and unstimulated cortex, would show an increased positive BOLD response that is the average of the responses in the stimulated and unstimulated regions, and would therefore be inordinately high because of the perfusion without concomitant oxygen consumption in flanking cortical regions. On the other hand, a SE BOLD response limited to the smaller veins in the stimulated cortex where perfusion and oxygen consumption are balanced would show an appropriately low positive BOLD response.

If the above model were true, then the SE BOLD response measured in the GE BOLD ROI should have the same non-linearity observed for the GE BOLD data in the GE BOLD ROI. The data from this experiment are inconclusive on this point: the amplitudes of the 5% contrast and 10% contrast SE BOLD HRFs in the GE BOLD ROIs were not significantly different, which could suggest the effect described above, but may simply be the result of low contrast-to-noise ratio for the SE BOLD experiment. The GE BOLD response in the more spatially selective SE BOLD ROI would not necessarily lack the low-contrast, localized non-linearity because extravascular effects from large veins can extend several millimeters in cortex. Again, the data from this experiment are inconclusive on this point, and further work is necessary to discover whether perfusion is broadly targeted for weak, isolated stimuli. However, one group, using optical imaging, has also found evidence consistent with increased sensitivity to weak neural activity in hemodynamic signals (Zhan, et al. 2005).

It is also possible that the non-monotonic increase in the GE BOLD response that we observe is not a failure of linearity in neurohemodynamic coupling, but rather a true reflection of non-monotonic neural response. Even though the stimuli were equated for

perceptual difficulty using separate staircases for each contrast level so subjects were detecting contrast increments with 80% accuracy for all pedestal contrasts, perhaps the sheer difficulty of reliably perceiving 5% contrast Gabors at 3° eccentricity resulted in a neural modulation akin to an attentional modulation (Buracas and Boynton). Robust V1 BOLD responses are known to represent perception, rather than actual stimulus presence or contrast (Ress and Heeger 2003; Maier, Wilke et al. 2008). An alternative explanation for the pattern of GE BOLD responses that we observed is that modulation of attention, in spite of the assigned contrast discrimination task, disproportionately amplifies the neural (and therefore BOLD) response at 5% contrast under the particular conditions of the experiment we conducted. If this is the case, it is again difficult to explain why the effect was observed in the GE BOLD signal but not in the SE BOLD signal. Using attention to explain the full pattern of results we observed would therefore requires invoking an attention-based non-linearity in the pooling of blood from small-diameter venous compartments to large-diameter venous compartments.

Unless an unknown effect of effort or attention exists that amplifies the GE BOLD response but not the SE BOLD response, as considered above, the SE BOLD technique appears in this study to be a more reliable indicator of the underlying neural activity. This improved functional specificity appears to apply only to the special case of small, low-contrast, isolated stimuli, but strengthens arguments in favor of using SE BOLD rather than GE BOLD for high-resolution studies of localized neural activity (Yacoub, Shmuel et al. 2007). Our data also demonstrate the primary limitations of SE BOLD techniques – decreased contrast-to-noise ratio. In one subject for the main experiment the SE BOLD responses were too weak to analyze, and in both experiments, several of the 5% contrast responses were undetectable. Furthermore, the low CNR made it difficult to distinguish between spatial selectivity and weak responses, given the practical limitations on the number of trials that could be presented in a single scanning session.

The volume of the SE BOLD-derived ROIs was about a third of the volume of the GE BOLD-derived ROIs. While the GE BOLD-derived ROIs were larger than our estimates for the volume of the cortical representation for a single Gabor, the dendritic arbors of pyramidal neurons in V1 can span a millimeter or more, and some estimates of neural point-spread functions suggest that the blurring of the neural signal across the cortical surface can be described by a Gaussian kernel with 2-3 mm full width at half-maximum (Amir, Harel et al. 1993; Grinvald, Lieke et al. 1994 1994; Angelucci, Levitt et al. 2002 Hupe, Bullier & Lund, 2002). Therefore, a 300 mm^3 volume for the GE BOLD ROIs may be a reasonable representation of the cortical response (i.e., ~10 mm diameter) with minimal contributions of vascular blurring. The smaller volume of the SE BOLD ROIs might then be attributed to the lower contrast-to-noise ratio in the SE BOLD data, which results in the selection of only the more strongly modulated voxels in the center of the cortical representation of each Gabor patch. This spatial bias may be one reason for the apparent improvement in linearity of the SE BOLD techniques for low-contrast stimuli – correspondingly, the GE BOLD nonlinearity was reduced in the more selective SE BOLD-derived ROI.

While the control experiment ruled out the possibility that the GE BOLD non-linearity is simply an artifact of experiment design, it is possible that the non-linearity is nonetheless a finding limited to the particular stimulus presentation paradigm studied in this experiment. This experiment used a rapid event-related paradigm (3-6 s inter-trial interval), with paired 250 msec presentations of Gabor patches separated by a 250 msec inter-stimulus interval. Further studies might test whether the observed non-linearity is present in a slow event-related design with single image presentations, and this is an interesting question from a mechanistic perspective. From a practical perspective, however, few studies of visual perception or human behavior have the luxury of slow event-related designs because of the difficulty subjects have in remaining alert during long stretches of inactivity and, for small stimuli, the need to acquire 50-100 repetitions

of a single stimulus condition in order to estimate reliable HRFs. Because this non-linearity does not exist for large stimuli, it is perhaps sufficient that this study provides a cautionary note regarding the lack of correspondence between GE BOLD responses and the V1 neural response to small, isolated, low-contrast visual stimuli presented in a rapid event-related paradigm.

Conclusion

For the special case of isolated, low-contrast Gabor elements presented at 3° eccentricity, the GE BOLD response is larger than predicted from psychophysical measurements of contrast discrimination thresholds. While this could represent a disproportionate contribution of attention to the neural representation of stimuli that are difficult to see in parafoveal regions, the apparent linearity of the relationship between the SE BOLD response and inferred neural activity leads us to conclude that the disproportionate GE BOLD response to low-contrast, isolated Gabor patches is a consequence of a vascular non-linearity. While it appears likely that the proposed nonlinearity would be encountered only rarely – it is not present at higher contrast or when stimuli are increased to subtend several degrees of visual angle – it is an important cautionary note for the interpretation of high-resolution BOLD measurements of the cortical representation of finely detailed visual stimuli.

Chapter 3

High-Resolution BOLD fMRI Measurements of Local Orientation-Dependent Contextual Modulation Show a Mismatch between Predicted V1 Output and Local BOLD Response

Authors: Jennifer F. Schumacher, Cheryl A. Olman

Vision Research 50 (2010) 1214-1224

Abstract

The blood oxygenation level-dependent (BOLD) functional MRI response to suppressive neural activity has not been tested on a fine spatial scale. Using Gabor patches placed in the near periphery, we precisely localized individual regions of interest in primary visual cortex and measured the response at a range of contrasts in two different contexts: with parallel and with orthogonal flanking Gabor patches. Psychophysical measurements confirmed strong suppression of the target Gabor response when flanked by parallel Gabors. However, the BOLD response to the target with parallel flankers decreased as the target contrast increased, which contradicts psychophysical estimates of local neural activity.

Introduction

Because many interesting details of neural coding are found on a fine spatial scale, the high spatial resolutions achievable in fMRI are attractive to many neuroscientists. The first goal of the experiments reported here was to accurately localize and analyze the blood oxygenation level-dependent (BOLD) response to a specific spatial location in a visual scene. This precise localization should provide a better interpretation

of the underlying neural activity. For example, our understanding of the neural processes associated with change blindness and many visual illusions would be improved by the ability to study responses to individual image features. Previous work has suggested that the spatial accuracy of GE BOLD is about 3.5 mm, based on the vascular point spread function (PSF) (Das & Gilbert, 1995; Engel, Glover & Wandell, 1997; Ogawa, Menon, Tank, Kim, Merkle, Ellermann & Ugurbil, 1993; Parkes, Schwarzbach, Bouts, Deckers, Pullens, Kerskens & Norris, 2005). For the neural response itself, smaller neural PSFs (2 - 3 mm) are expected based on the spatial extent of horizontal connections and dendritic arbor geometry (Angelucci, Levitt, Walton, Hupe, Bullier & Lund, 2002; Amir, Harel & Malach, 1993; Grinvald, Lieke, Frostig & Hildesheim, 1994). Here we investigate whether the BOLD responses to clusters of neural activity approximately 5 mm apart on the cortex can be distinguished reliably and whether suppression by parallel context is apparent in the BOLD signal.

Studying surround suppression with BOLD fMRI on a local scale will allow further insight into how humans view and parse visual scenes by studying how context modulates the response to individual features. Inhibition is a fundamental aspect of visual processing, playing a role in neural computations both between and within cortical areas of the brain. To investigate the BOLD response to local inhibition, we use surround suppression, which has been studied extensively (a selection pertinent to our research: (Cavanaugh, Bair & Movshon, 2002; Polat, Mizobe, Pettet, Kasamatsu & Norcia, 1998; Zenger-Landolt & Koch, 2001) and is strong in the near periphery (1°- 4° eccentricity) (Petrov, Carandini & McKee, 2005; Xing & Heeger, 2000). In both electrophysiological (Cavanaugh et al., 2002) and psychophysical (Zenger-Landolt & Koch, 2001) experiments, a stimulus with a parallel surround exhibits a suppressed neural response compared to the stimulus alone, and an orthogonal surround results in either weaker suppression or facilitation.

Literature reports on the BOLD response to neural suppression conflict, claiming

either an increase or a decrease in the BOLD response during neural suppression. Several studies show a decrease in the BOLD response with neural inhibition (Chen, Silva, Yang & Shen, 2005; Devor, Tian, Nishimura, Teng, Hillman, Narayanan, Ulbert, Boas & Kleinfield, 2007; Northoff, Walter, Schulte, Beck, Dydak, Henning, Boeker, Grimm & Boesiger, 2007; Shmuel, Augath, Oeltermann & Logothetis, 2006; Zenger-Landolt & Heeger, 2003). However, there is also work that predicts an increase in the BOLD response with neural inhibition (Ackermann, Finch & Babb, 1984; Cauli, Tong, Rancillac, Serluca, Lambolez, Rossier & Hamel, 2004; Lauritzen, 2001; Nie & Wong-Riley, 1995; Pelled, Bergstrom et al. 2009). When responses are measured over a large cortical area, a comparison of visual psychophysics and BOLD fMRI finds that neural suppression induces a decrease in the BOLD response (Pihlaja, Henriksson, James & Vanni, 2008; Zenger-Landolt & Heeger, 2003). The experiments described here use a flanking inhibition paradigm with single target Gabor patches to test whether the BOLD response decreases when a parallel surround suppresses neural activity. Our data show that the localized BOLD response does not match the inferred local neural activity, indicating that the BOLD response can not always be simply predicted by the response in neurons turned to the presented stimulus and suggesting that more complex models of neurohemodynamic coupling may be required to interpret BOLD response of individual image features in a complex context.

Materials and Methods

Subjects

We performed three separate experiments, and each experiment's data were collected from three human subjects from a pool of five subjects (four female, age 21 – 36, mean age 27.6) with normal or corrected to normal vision. The experimental protocols conformed to safety guidelines for MRI research and were approved by the

Institutional Review Board at the University of Minnesota. Subjects provided written informed consent before participating in the experiments.

Visual Stimuli

The targets-alone stimuli for the first experiment (Figure 3.1A, top) consisted of four Gabor patches located in each of the four visual quadrants at 3° eccentricity. Each Gabor patch consisted of a 3 cycles-per-degree (cpd) sinusoidal grating modulated by a Gaussian envelope with full width at half-maximum of 0.6° (σ = 0.25°). The contrast response stimuli (second experiment) were the same as the targets-alone condition in the target and flankers experiment; however the orientation of the sinusoidal grating was randomized for each Gabor patch during each interval to avoid adaptation.

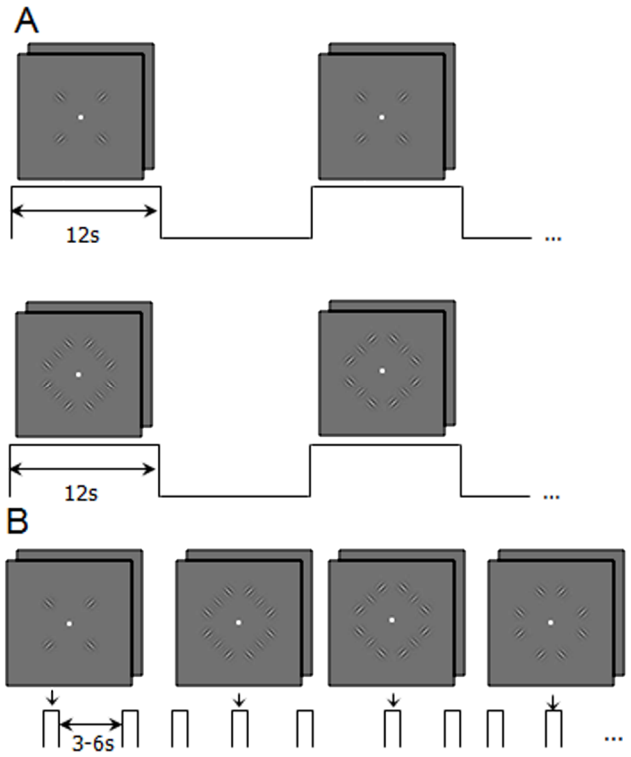

Figure 3.1: Stimuli used to study contextual modulation in V1. (A) Targets alone (top) and targets with flankers (bottom) block localizer scans. Stimuli were presented in the same 2IFC paradigm, 6 trials per 12 second block. During "blank" blocks subjects performed a 2IFC contrast detection task with a 0% target pedestal contrast. Ten and one half cycles were completed per scan. (B) Stimuli for

event related scans: targets with parallel flankers (target contrast was 8%, 16%, or 32%), targets with orthogonal flankers (again, target contrast was 8%, 16%, or 32%), targets alone (32% contrast on all trials), and flankers alone (50% contrast). Stimuli were presented in a 2-interval forced choice (2IFC) paradigm (stimulus duration: 250 ms, inter-stimulus interval (ISI): 500 ms) Inter-trial interval was 3, 4.5 or 6 seconds (randomly selected for each trial).

In the first experiment, (the main experiment, measuring the BOLD response to the target Gabors with parallel and orthogonal context), flanking Gabor patches were located on either side of the target Gabor with a center-to-center distance of 1° between target and flanker. Flankers were always presented at 50% contrast and were oriented either orthogonal to or parallel to the target Gabor. Stimuli for both the target and flankers experiment and the contrast response to targets-alone stimuli were displayed on a NEC 2180UX LCD monitor, subtending 8° x 11° of visual angle at a viewing distance of 200 cm.

The annulus stimuli (third experiment) were modeled after the center/surround stimulus used in Zenger-Landolt and Heeger, 2003. The central annulus extended from 2° to 4° eccentricity and the surround extended from 0.5° to 2° and from 4° to 8° eccentricity. Both the central annulus and the surround consisted of a 2 cpd sinusoidally modulated luminance grating. The orientation of the gratings changed after each trial and the gratings were contrast reversing at a rate of 4 Hz to avoid adaptation. The surround was always presented at 100% contrast and was oriented parallel to the central annulus. Stimuli were projected by a Sanyo (Sanyo North America Corporation, San Diego, CA, USA) projector with a custom zoom lens (NuView lens by Navitar, Rochester, NY, USA), housed outside the magnet room, onto a screen placed in the back of the magnet, and viewed from a mirror over the subjects' eyes.

All stimuli were presented on a mean gray background. Stimuli were generated and presented with Matlab (Mathworks, Inc., Natick, MA) and Psychtoolbox (Brainard, 1997; Pelli, 1997). Macintosh G4 computers with OS X served as the processors for the psychophysics and fMRI systems.

Psychophysics

Contrast response functions for three stimulus configurations (targets-alone, targets with parallel flankers, and targets with orthogonal flankers) were estimated from contrast discrimination thresholds. For these psychophysical measurements, a Bits++ digital video processor (Cambridge Research Systems Ltd., UK) was used with the LCD monitor to provide 14-bit brightness resolution. Eight pedestal contrasts were employed for the target Gabor patches: 0%, 1%, 2%, 4%, 8%, 16%, 32%, and 64%. On each trial, all four targets appeared. On one of the two intervals in the trial, one of the four targets was incremented in contrast. The stimulus was presented for 250 ms in each interval, with a 500 ms blank inter-stimulus interval. Subjects maintained fixation on a white square at the center of the stimulus set while indicating the interval (1 or 2) in which one of the target Gabors increased in contrast; feedback for the task was given by a green ('correct') or red ('incorrect') color at fixation after each response. A 3-down 1-up staircase was used to control the contrast increment on each trial; this staircase converged at a performance level of 79% correct, which was used as the threshold estimate for each pedestal contrast for each stimulus condition. Five threshold estimates (5 runs of 40 trials) at each of the eight contrast levels for each condition (targets-alone, targets with orthogonal flankers, and targets with parallel flankers) were completed per subject.

Threshold versus contrast (TvC) curves for each condition and each stimulus type were fit (using Matlab's lsqcurvefit function) with a variant of the Naka-Ruston formula (Equations 3.1 and 3.2, see (Zenger-Landolt & Heeger, 2003)). The extra parameters in this fit allow for the fact that flankers suppress the target response when target contrast is lower than flanker contrast, but flankers become consistently facilitative when the target contrast is greater than the flankers. The inferred contrast response function for each stimulus configuration was the integral of this function. Parameters used to fit the data from Subject 2 (Figure 3.2, middle column) are shown in Table 3.1.

Equation 3.1: $r(x) = ax^p / (x^{p-q} + b^{p-q})$

Equation 3.2: $x(c) = dc + ec^f$

Table 3.1: Parameter values implemented to fit the TvC curves with Equations 1 and 2 for psychophysics results for Subject 2 presented in Figure 3.2 (middle column).

	a	b	d	e	f	p	q
Target	35	109	84	0.20	2.6	1.7	0.32
Target with parallel flankers	47	147	112	0.22	3.5	1.6	0.19
Target with orthogonal flankers	46	178	148	0.36	2.7	1.8	0.25

fMRI Experiments

The target and flankers BOLD fMRI experiment (Experiment 1) was completed on a Siemens Trio 3T system (Siemens, Erlangen, Germany) at the Center for Magnetic Resonance Research at the University of Minnesota. The scanner was equipped with Sonata gradients (maximum amplitude: 40 mT/m; slew rate: 200 T/m/s). An eight-channel RF head-coil was used to acquire gradient echo (GE) EPI images. Field of view was 192 mm x 144 mm with a matrix size of 128 x 96 (6/8 partial Fourier acquisition) for a nominal inplane resolution of 1.5 mm isotropic. Slice thickness was 1.5 mm, volume repetition time (TR) was 1.5 s and echo time (TE) was 30 ms. Seventeen slices were prescribed perpendicular to the calcarine sulcus in an oblique coronal orientation and covered early visual areas.

For the target and flankers experiment, each subject completed four scanning sessions on separate days. One session was for standard retinotopic mapping and acquisition of an MP-RAGE anatomy (1 mm isotropic resolution). The remaining three sessions each included three target localizer scans (block design, Fig. 1A top), three target with flankers (superset) localizer scans (block design, Fig. 1A bottom), and three event-related scans (Fig. 1B).

Targets were presented at 32% contrast in the block localizer scans. For the targets-alone localizer, subjects performed a contrast discrimination task as in the psychophysical measurements. During “on” blocks the target pedestal contrast was 32%;

during “off” blocks the target pedestal contrast was 0%. On and off blocks each lasted 12 s; 11 on blocks alternated with 10 off blocks during each scan, and the first on block was discarded before analysis. The superset localizer scans had the same block design, but subjects performed a contrast-matching task during the “on” blocks. Targets with orthogonal flankers were presented in one of the two intervals, and targets with parallel flankers were presented in the other. Subjects indicated the interval (1 or 2) in which the targets appeared to have higher contrast. Target contrast was adjusted on a staircase throughout the scan, converging at a contrast at which the targets with parallel flankers appeared to have the same contrast as with orthogonal flankers. On average, subjects required a 10% contrast increment before reporting matched perceived contrast for the two conditions; this approximately matched estimated contrast response functions from the psychophysical sessions. During the “off” blocks, subjects were engaged in a detection task for the targets-alone stimuli (all four were incremented together, as in the “on” blocks).

The event-related scans measured the BOLD response to eight stimulus conditions: targets-alone, flankers-alone, and six targets-with-flankers conditions. In the targets-alone condition, targets were presented with 32% contrast. In the flankers-alone condition, orthogonal flankers were used on half of the trials and parallel flankers on the rest. For the remaining six conditions, targets were presented at three contrast levels (8%, 16%, and 32%) with either parallel or orthogonal flankers. Flankers were always presented at 50% contrast. In the event-related scans, stimuli were presented with the same timing as in the psychophysical measurements and subjects were engaged in the same two-interval forced choice contrast discrimination task as in the psychophysics. Pairs of stimuli were presented with an inter-trial interval of 3, 4.5 or 6 s (inter-trial interval was randomly selected and uniformly distributed). Separate adaptive staircases were used to equate task demands between conditions; the flankers-alone conditions used a contrast detection task with 0% pedestal contrast targets. There were a total of 88 trials

per scan (11 of each stimulus type), for a total of 33 presentations of each stimulus type on each day. Subjects viewed the stimuli via a mirror mounted on the head-coil; behavioral responses were collected using a fiber-optic button box (Current Designs, Philadelphia, PA).

The contrast response and annulus BOLD fMRI experiments (Experiments 2 and 3) were completed on the same magnet after it had been upgraded to a Siemens TIM Trio 3T system (Siemens, Erlangen, Germany) with Avanto gradients (maximum amplitude: 45 mT/m, slew rate: 200 T/m/s). A 12-channel RF receive-only head-coil was used to acquire the GE EPI images with a TR of 1.5 s and TE of 30 s. For the contrast response data (Experiment 2), the field of view was 256 mm x 256 mm with a matrix size of 128 x 128 for a nominal inplane resolution of 2 mm isotropic. Eighteen slices (2 mm slice thickness) were aligned perpendicular to the calcarine sulcus in an oblique coronal orientation covering early visual areas. For the annulus experiment (Experiment 3), the field of view was 192 mm x 192 mm with a matrix size of 64 x 64 for a nominal inplane resolution of 3 mm isotropic. Twenty-five slices (3 mm slice thickness) were aligned perpendicular to the calcarine sulcus in an oblique coronal orientation covering early visual areas.

For the contrast response experiment, two subjects participated in three scanning sessions each and the third subject participated in one scanning session. Each scanning session involved at least four functional localizers and three event-related scans. (The first two subjects participated in three scanning sessions because each session included eight additional block-design scans to estimate the contrast response function, and therefore only three or four event-related scans. The third subject participated in a scanning session with only four block-design localizers and six event-related scans.) Anatomical and retinotopic information were used from a previous scanning session. The contrast response scans were similar to the event-related target and flanker experiment, except the only stimulus was targets-alone, presented at 8%, 16%, and 32% pedestal

contrast. There were 15 trials of each contrast level per scan, for a total of at least 75 trials per scanning session. Block-design functional localizers, similar to Experiment 1, were used to define the target-alone ROIs, except with only eight "on" blocks and seven "off" blocks (each block lasting 12 s) per scan.

For the annulus experiment, each subject participated in one scanning session, which involved at least two central annulus localizer scans (differential block design) and at least six event-related scans (at least four scans with-surrounds and at least two scans without-surrounds). Anatomical and retinotopic information were used from a previous scanning session.

In the differential block localizer scans, the central annulus and the surround were presented at 100% contrast with a 50% duty cycle (0.75 s of 4 Hz contrast-reversing grating interleaved with 0.75 s of mean gray screen with a persistent fixation mark and black outline defining the annulus region divided into eight equal subregions). Subjects performed a contrast discrimination (central-annulus-alone blocks) or contrast detection (surround-alone blocks) task in which the contrast of one of the eight segments of the central annulus decreased (discrimination task) or increased (detection task) from the pedestal contrast on half of the trials. On and off blocks each lasted 12 s; 11 on blocks alternated with 10 off blocks during each scan, and the first on block was discarded before analysis.

Two different event-related scans were used to measure the BOLD response to the center annulus with and without-surrounds. The experiment design was modeled after Zenger-Landolt and Heeger (2003), but adapted to an event-related paradigm with the same stimulus presentation timing as the targets and flankers experiment. In the with-surrounds scan, the surround annuli were presented at a 50% duty cycle throughout the entire scan (present for 0.75 s, every 1.5 s). This design ensures that the measured hemodynamic response reflects the BOLD response to the center annulus itself, and is robust against hemodynamic suppression effects that may result from the extended

surround grating. Three stimulus conditions were measured in the with-surrounds scans: 10%, 20%, and 40% contrast annulus with parallel surrounds. Surrounds were always 100% contrast. In the without-surrounds scans, two conditions were measured: the center annulus alone (40% contrast) and surround-alone (100% contrast). In all event-related scans, the stimuli were presented for 0.75 seconds with an inter-trial interval of 3, 4.5 or 6 s (inter-trial interval was randomly selected and uniformly distributed). A contrast discrimination task was used in which one of the eight segments of the central annulus decreased in contrast during half of the trials, except during the surround-only condition, in which a contrast detection task was employed since the central annulus was at 0% pedestal contrast. The fixation mark provided correct or incorrect feedback for the task by turning green or red, respectively. There were a total of 60 trials for each stimulus condition per scanning session (four with-surrounds scans with 15 presentations of each stimulus type, and two without-surrounds scans with 30 presentations of each stimulus type).

fMRI Data Analysis

Preprocessing of functional data, which included motion compensation, high-pass filtering, and alignment of functional data to the reference anatomy (Nestares & Heeger, 2000), was accomplished with custom Matlab code. Fieldmap-based distortion compensation for the EPI images was completed with FSL (Smith, Jenkinson, Woolrich, Beckmann, Behrens, Johansen-Berg, Bannister, De Luca, Drobnjak, Flitney, Niazy, Saunders, Vickers, Zhang, De Stefano, Brady & Matthews, 2004). For the reference anatomy, gray/white matter segmentation, cortical surface reconstruction and surface inflation and flattening were completed in SurfRelax (Larsson, 2001). Standard retinotopic mapping (DeYoe, Carman, Bandettini, Glickman, Wieser, Cox, Miller & Neitz, 1996; Engel et al., 1997; Sereno, Dale, Reppas, Kwong, Belliveau, Brady, Rosen & Tootell, 1995) using rotating wedges and expanding rings was used to identify V1 and

an iso-eccentricity band centered at 3° of visual angle from the fovea. Boundaries for visual areas were translated to the reference anatomy, and from there to the functional data, to restrict where ROIs would be defined for further analysis.

For each target and flankers and contrast response scanning session (Experiments 1 and 2), ROIs were selected based on retinotopic location and functional localizers. Voxels within the pre-selected 3° eccentricity band in V1 with coherence exceeding 0.15 (Bandettini, Jesmanowicz, Wong & Hyde, 1993; Engel et al., 1997) during the appropriate localizer (target or superset) were initially defined in the flat cortical representation and then translated to the inplane anatomy for selection of only contiguous voxels. A phase window from about π to 1.6π was used to select BOLD responses that were positive when the stimulus was present. Similarly, for the contrast response data, voxels within this same retinotopic area but exceeding a coherence of 0.3 during the functional localizers were used for the ROI. (A larger coherence threshold was used for Experiment 2 because more functional localizer scans were available per subject.)

A general linear model (GLM) was used to analyze the event-related data. Custom Matlab code estimated the amplitude of the BOLD response for 12 time points (18 s) after the stimulus onset to avoid making assumptions about the shape of the hemodynamic response function (HRF). Multiple scans from a given scanning session were concatenated in time and a single HRF was estimated for each stimulus type for each scanning session. Hemodynamic responses were characterized either by the peak amplitude of the response (4.5 s after the stimulus onset) or by the amplitude of a difference-of-gamma functions HRF model fit to the data. Both methods produced identical results for the overall pattern of BOLD responses. For the target and flankers experiment, BOLD response amplitudes were calculated for individual subjects (3) on separate days (3), and then averaged (for n = 9).

The contrast response data were motion compensated with FSL's MCFLIRT function (Jenkinson, Bannister, Brady, & Smith, 2002), but otherwise used the same

preprocessing steps and GLM analysis as the target and flankers experiment. Fifteen percent of the highest variance voxels were removed from the ROI to eliminate voxels dominated by large vessels (Olman, Inati, & Heeger, 2007) and thereby minimized localization errors. The contrast response hemodynamic response estimates were averaged across scanning sessions for each subject: three sessions (20 total event-related scans for the first subject), three sessions (12 total event-related scans) for the second, and one session (nine event-related scans) for the third.

The same preprocessing and GLM methods were used for the annulus fMRI experiment, except distortion compensation was not used. ROIs were defined based on retinotopic information and the differential block localizers. Voxels within the pre-selected 2° - 4° eccentricity band in V1 with coherence exceeding 0.3 (Bandettini, Jesmanowicz, Wong & Hyde, 1993; Engel et al., 1997) during the functional localizer were initially defined in the flat cortical representation and then translated to the inplane anatomy for selection of only contiguous voxels. A separate ROI was created for each hemisphere for each subject, totaling n = 6 for the final analysis. Fifteen percent of the highest variance voxels were removed from the ROI to eliminate voxels dominated by large vessels. The difference-of-gamma HRF fits were determined per hemisphere and then peak amplitudes were averaged.

Expected size of cortical representation of stimuli

As a rough estimate of the size of the cortical territory representing each individual Gabor patch, the functional form for human cortical magnification estimated by Engel et al. (1997) was used:

$$E = e^{.063*(x + 36.54),} \qquad \text{or} \qquad x = (\ln(E)/0.063) - 36.54$$

where x is cortical distance in millimeters (from the cortical location where 10° eccentricity is represented), and E is eccentricity. A Gabor patch that is 0.6° wide (FWHM) at 3° eccentricity therefore extends from -21 to -17.5 mm on the cortex (in a

radial direction). Assuming roughly symmetric cortical representation and constant cortical thickness, the neural representation of the Gabor is estimated to occupy a cylindrical cortical territory described by a circle with radius 3.5 mm, projecting through the depth of the gray matter (approximated as 3 mm on average, for a total cortical volume of 115 mm^3, or 34 1.5 mm isotropic voxels). Following the same logic, the central annulus for Experiment 3 occupies a band of cortex with a width of 11 mm, projecting through the depth of the gray matter.

Results

Psychophysics

To confirm suppression of the neural response to target stimuli in the presence of local parallel context, we measured contrast discrimination thresholds as a function of target pedestal contrast for three stimulus conditions: targets with orthogonal and parallel flankers, in addition to targets-alone (Fig. 3.1). The flanking Gabor patches were always presented at 50% contrast, for both the psychophysical measurements and for the subsequent BOLD experiment. In the psychophysical measurements, we found suppression for both the orthogonal and parallel conditions compared to the targets-alone responses, with more suppression for the parallel configuration (Fig. 3.2), consistent with {Zenger-Landolt & Koch, 2001}. Behavioral data from the fMRI experiments revealed a similar pattern of responses, albeit with smaller thresholds, most likely because there were only 11 trials per scan and the contrast increment started low (data not shown).

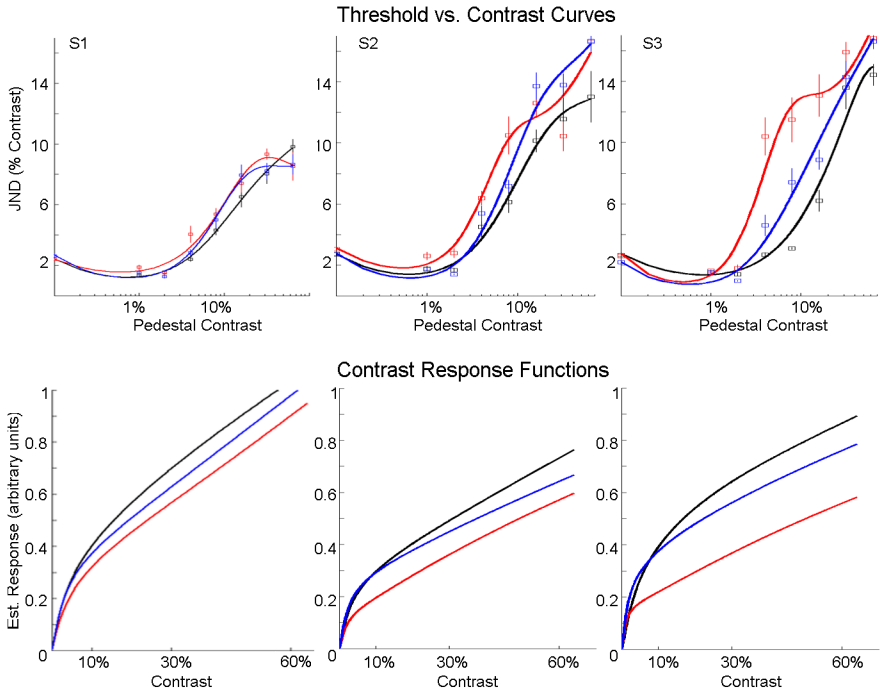

Figure 3.2: Psychophysical quantification of suppression of target Gabor responses by flanking Gabor patches. The top row has threshold versus contrast plots (red: parallel flankers, blue: orthogonal flankers, black: targets alone) while the bottom row shows inferred contrast response functions (calculated after fitting threshold versus contrast data with a variant of the Naka-Rushton formula, equations 1 and 2). Each column contains the result from a single subject. High contrast discrimination thresholds for the targets with parallel and orthogonal flankers translated to a low inferred neural response in the contrast response function (CRF) compared to the targets-alone configuration for all three subjects. Psychophysical measurements predict parallel flankers will suppress neural response to target Gabors 20 – 50% when the targets are at 16% contrast.

Localization of Specific Spatial Locations

To localize specific cortical regions of interest (ROIs), two separate arrangements of Gabor patches were used as visual stimuli (Fig.1A): a targets-alone stimulus and a targets-with flankers-stimulus. A target ROI set consists of four sub-ROIs representing the four target locations. A superset ROI set consists of the four regions of cortex responding to the four sets of targets and flankers (both orientations of flankers were used for the localizer). Each stimulus (targets-alone and targets-with-flankers) was used in a separate block design localizer as described in the Methods section.

Results from the block localizer scans are summarized in Figure 3.3. The definition of both the target and the superset (targets-with-flankers) ROIs is shown for a representative subject (Fig. 3A). The average response of each target component ROI (single Gabor patch) was a volume of 28 (1.5 mm isotropic) voxels; the average volume of each superset component ROI (three Gabor patches) was 81 voxels. Predicted ROI volumes based on typical cortical magnification factors in humans were 34 voxels for each component of the target ROIs, and 102 voxels for each component of the superset ROIs.

The repeatability of localization of a particular spatial location in the visual field over three scanning sessions is shown for a single subject in Figure 3.3B. ROIs from each day (session) were translated to the volume anatomy, and each session's target ROI is outlined in a different color. Some errors in ROI definition and/or alignment are obvious – for example, the Day 1 ROI (blue outline) contains a significant amount of white matter. This is likely due to an imperfect registration between the functional and anatomical data for that data set. To illustrate variability across the entire experiment, the volumes and centers of mass for each target ROI for each day in each subject are shown in Fig. 3C. We quantified the precision of our spatial localization by averaging the three-dimensional cortical distances between each center of mass for each component ROI over the three days in the volume anatomy. The average Euclidean distances and standard error of the mean between individual day target ROI centers of mass were 2.11 mm ± 0.27, 3.82 mm ± 0.55, and 3.28 mm ± 0.53 for the three subjects.

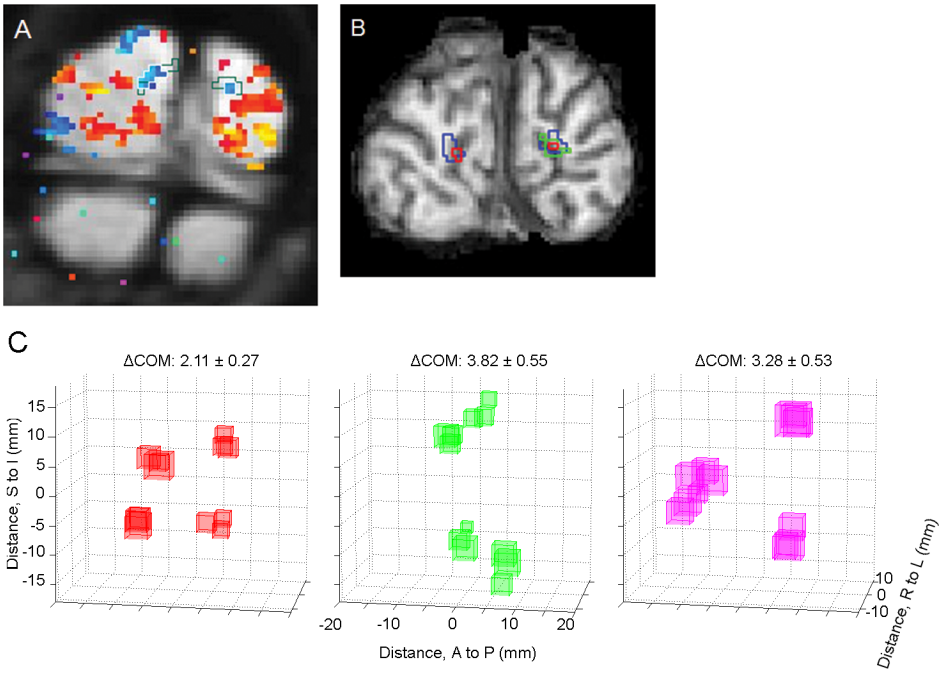

Figure 3.3: ROI localization. (A) Functional data from target block localizers (averaged data from three days, a total of 9 target-alone localizer scans), for one subject (S3), overlaid on mean functional image (color map: blue indicates in-phase with stimulus presentation, red indicates out of phase with stimulus presentation). Target ROI is indicated by white outline, superset ROI (identified by a different set of functional data) is indicated by dark green outline. Two of four sub-ROIs are visible in this particular slice; the other two sub-ROIs are located in different slices. (B) Target ROIs from three different days for the same subject, translated to the reference anatomy (1 mm isotropic resolution) and shown on a single coronal slice (Blue: Day 1, Green: Day 2, Red: Day 3). (C) Three-dimensional plots of all target ROI locations for all subjects for three days. For each subject, each sub-ROI is represented by a cube centered at the calculated center of mass (COM). The volume of the cube indicates the volume of the sub-ROI. Indicated above each plot is the average pairwise 3D Euclidian distance between sub-ROI COMs from the three different days (n=12 comparisons, 3 for each of 4 locations, for each subject).

BOLD Response to Contextual Modulation

Three scans with an event-related design were also completed during each scanning session for Experiment 1, using a total of eight stimuli: targets-alone, targets with parallel flankers for three different target contrasts (8%, 16%, 32%), targets with orthogonal flankers for three different target contrasts (8%, 16%, 32%), and flankers-alone (in the orthogonal configuration on half of the trials, and in the parallel configuration on the other half). Flankers were always presented at 50% contrast. Using

ROIs determined from both the target and the superset block localizers, HRFs were estimated for 12 time points (18 s) following stimulus onset.

Figure 3.4 shows HRFs in the target ROI for all conditions for one subject's average BOLD response over three scanning sessions. Even with blurring due only to motion compensation for a single day, the BOLD response in the target ROI contains a strong contribution from the flankers – the flankers-alone response (green line, Fig. 4A) is not only apparent in the target ROI, but is also among the largest in amplitude (even though the target stimulus is not present). This result might be predicted from blurring of the hemodynamic and/or neural responses. As a further indication of significant blurring in the hemodynamic response, the pattern of results in the target ROI (Fig. 4D, described below) was the same as the pattern of results in the superset ROI (Fig. 4E).

Significant and opposite patterns were found for the orthogonal and parallel conditions as a function of target contrast. For the orthogonal condition, the peak BOLD response increased as the target contrast increased (Fig. 4B & 4D). For the parallel flanker condition, the amplitude of the BOLD response decreased as the target contrast increased (Fig. 4C & 4D). The interaction between the orthogonal and parallel conditions was significant ($F_{2,48} = 3.41$, $p = 0.041$, two-way ANOVA). The superset ROI also had a significant result for this comparison ($F_{2,48} = 5.4$, $p = 0.008$, two-way ANOVA).

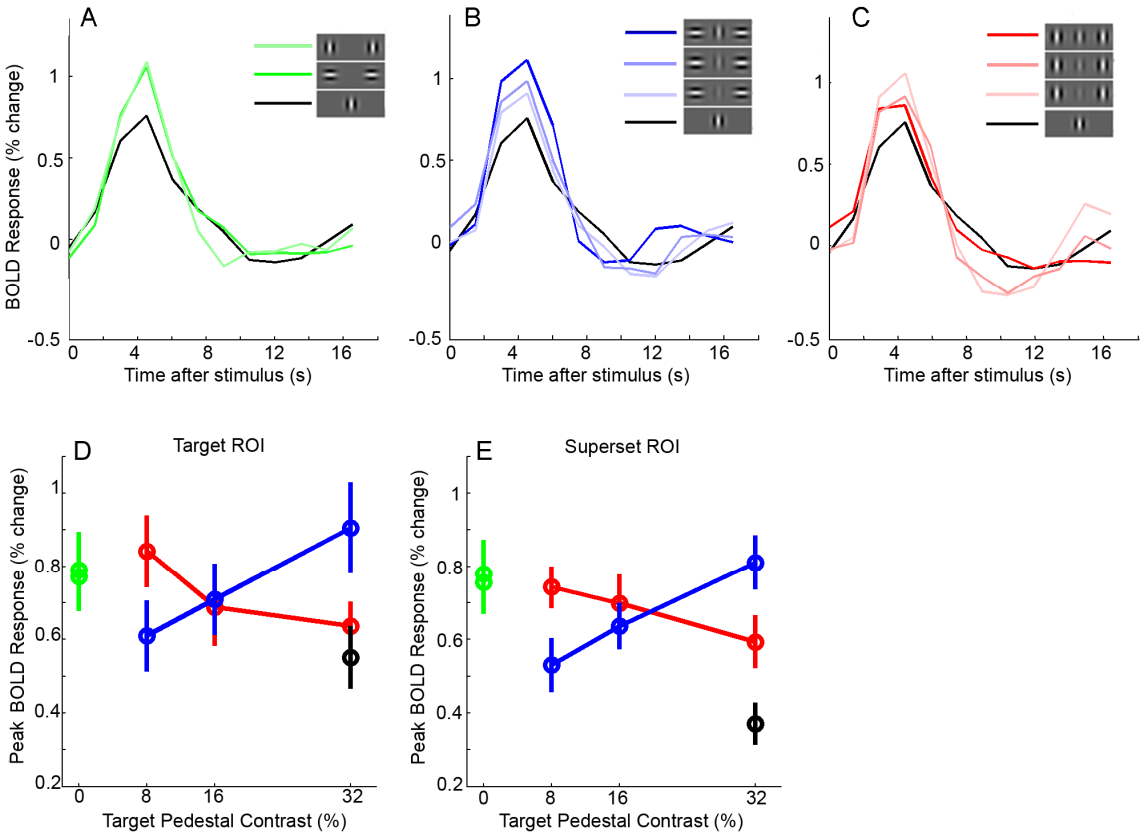

Figure 3.4: Estimated BOLD fMRI responses in target ROI. (A-C) BOLD fMRI responses from one subject (S1), averaged over three scanning sessions. Target-alone condition is shown in black. (A) In the target ROI, the flanker-alone conditions (green lines) dominate even though no target Gabor patch is present. (B) Peak BOLD response increases with an increase in target contrast with orthogonal flankers. (C) Peak BOLD response decreases with an increase in target contrast with parallel flankers. (D-E) Response amplitude is estimated as the amplitude of a difference-of-gamma functions HRF model fit to the estimated HRFs, and error bars represent SEM. Significant interaction was found between the parallel and orthogonal conditions ($p < 0.05$, 2-way ANOVA). (D) Summary of peak BOLD amplitude over all subjects, target ROIs (individual day data, n=9). (E) Summary of peak BOLD amplitude over all subjects, superset ROIs (individual day data, n=9). Similar patterns of results were obtained for both the target (D) and superset (E) ROIs.

A decrease of the BOLD response with increasing target contrast is not expected -- the target response is expected to be suppressed but increasing with contrast – however this pattern might be explained if (1) the BOLD response represents the sum of the target and flanker responses and (2) the response to the flankers is increasingly suppressed by the increasing target contrast. To test for this possibility, two of the subjects participated

in a psychophysical experiment in which contrast discrimination thresholds were measured for the parallel flanking Gabors while the target contrast was varied. (Aside from the change in response target, stimuli and methods were identical to the psychophysical measurements of contrast discrimination thresholds for the target Gabors.) We measured discrimination thresholds for the parallel and orthogonal flankers with target contrast at 8%, 16% and 32% while the flankers' pedestal contrast was always 50%. As shown in Figure 3.5, discrimination threshold decreased with increasing target contrast for both subjects. The logic generally used to link discrimination threshold measurements and neural (and BOLD) responses is that the threshold (just noticeable difference) is inversely related to the derivative of the neural response. The decreased threshold that we measured therefore indicates an increased slope of the neural response, which is consistent with facilitation rather than suppression. The model reported by Zenger-Landolt and Koch (2001) also predicts facilitation because the flanker contrast is higher than the target contrast. Therefore, the decrease of the BOLD response to the parallel configuration with increasing target contrast is not likely explained simply by dominance of the target ROI by flanker responses which are decreasing with increasing target contrast.

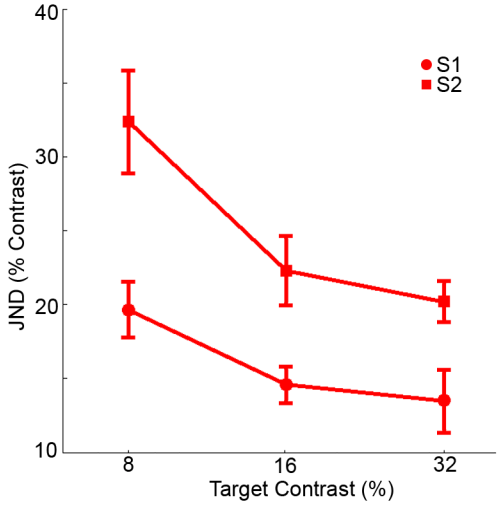

Figure 3.5: Discrimination thresholds for parallel flankers with 50% pedestal contrast, under three different target contrast conditions (8%, 16%, 32% pedestal contrast); error bars are SEM (n = 3

threshold estimates per subject). Thresholds decreased with increasing target contrast for both subjects, which would not be the case if flanker response was suppressed by targets of higher contrast.

To ensure that the pattern of results in the target and flankers experiment was not a consequence of a general decoupling between the BOLD response and the neural response at a local scale, we measured the BOLD contrast response function to the target-alone stimulus (Fig. 6). In an event-related design, the target-alone stimulus was presented at 8%, 16%, and 32% pedestal contrast. We confirmed a linear BOLD contrast response for these target-alone pedestal contrast levels: the BOLD response increased with increasing contrast. Therefore, the high-resolution BOLD contrast response function behaves monotonically as it does in low resolution and larger stimulus experiments (e.g. Boynton, Demb, Glover & Heeger, 1999).

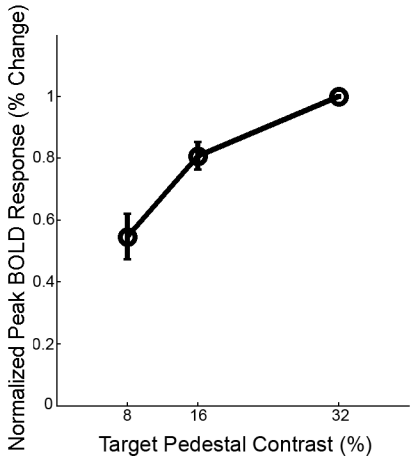

Figure 3.6: BOLD response to target-alone Gabor patches at 8%, 16%, and 32% pedestal contrast. Contrast response functions for individual subjects were normalized by the response to the 32% contrast stimulus and averaged (n = 3, error bars indicate SEM).

Additionally, to ensure that the pattern of results in the target and flankers experiment was not an artifact of the fast-paced event-related design we measured orientation-dependent suppression of a large annulus with an orthogonal or parallel surround in the same event-related design (Fig. 3.7). We measured 21% suppression with parallel surrounds compared to the central-annulus-alone response and an increase in BOLD response with an increase in the central annulus with parallel surrounds pedestal

contrast ($F_{2,15}$ = 3.53, p = 0.055). The increasing contrast response in the parallel condition is what is expected for surround suppression and what we failed to find with the target and flankers experiment.

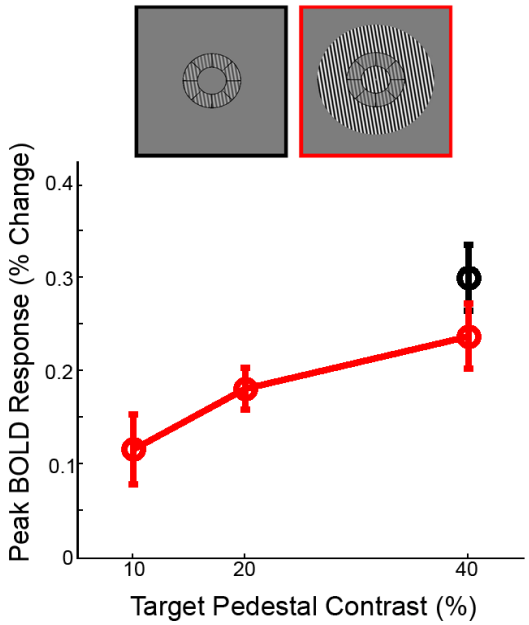

Figure 3.7: Annulus experiment results: BOLD response to the center annulus increases with increasing contrast, in spite of the presence of the parallel surround. Error bars represent SEM (n=6 hemispheres). The response to a 40% contrast center annulus is suppressed 21% by the presence of a parallel surround.

Discussion

By measuring localized BOLD responses to individual visual features with different local image contexts, we have found that responses to individual features can be localized with good precision across multiple days, but that even well-localized BOLD responses in V1 do not correlate with the suppression of V1 output that can be inferred by psychophysical measurements (and is reported in the electrophysiological literature). This finding can be interpreted in many ways, as discussed below. These interpretations range from mechanistic explanations (e.g., a dominance of inhibitory interneurons in regulating the hemodynamic response under our stimulus conditions) to the conclusion that the neural model we used to predict the BOLD data was insufficient (e.g., perhaps we failed

to incorporate sufficiently complex neural responses in the model of the underlying neural activity). But the basic value of the main experiment is that it defines at least one stimulus condition in which the models of neural response and neurohemodynamic coupling that successfully predict the BOLD response to large stimuli are insufficient for high-resolution measurements of small image features.

Psychophysical measurements of contrast discrimination thresholds were used to estimate the magnitude of neural activity in V1. In previous studies with a similar approach (Boynton, et al., 1999; Zenger-Landolt & Heeger, 2003), the agreement between the magnitude of the BOLD response and the similarly estimated V1 neural response was good, even under conditions of strong suppression. Using center-surround stimuli composed of extended sine gratings, we did measure good agreement between BOLD and psychophysical estimates of surround suppression (Experiment 3), but in our main experiment this agreement between BOLD and estimated V1 response was not found. For a target Gabor at 3° eccentricity, psychophysical measurements indicate that parallel flanking Gabor patches suppress the V1 neural response (Cavanaugh, et al., 2002 and our data, Fig. 2), but the suppressed neural response to the target Gabor patch nonetheless increases with increasing contrast. However, in a well-localized target ROI we measured the opposite pattern: adding suppressive flankers increased the response in the target ROI (which could be explained by blurring), and the BOLD response decreased with increasing target contrast in the parallel condition (a pattern that cannot be explained by blurring). The primary difference between the data reported here and previous studies showing good agreement between BOLD and neural response suppression (Boynton et al., 1999; Kastner, De Weerd, Pinsk, Elizondo, Desimone & Ungerleider, 2001; Pihlaja et al., 2008; Williams, Singh & Smith, 2003; Zenger-Landolt & Heeger, 2003) is the spatial scale over which the responses were measured.

Spatial accuracy of this experiment

Just as blurring of the signal cannot explain our results because the pattern was basically independent of voxel selection, localization errors cannot explain our pattern of results. Nonetheless, it is important to understand the limits of our ability to localize individual image elements. We found that our day-to-day ROI localization was accurate to within several millimeters, which puts an upper limit on our localization errors. Some of these errors are due to errors in the alignment between the functional and anatomical data (e.g., the Day 1 outline appearing in the white matter when resampled from the functional data). Those alignment errors would not affect our conclusions because hemodynamic response functions were estimated from ROIs defined in the functional data space for individual subjects on individual days. Still, we could have small localization errors on individual days. The contrast-to-noise ratio in the target localizer data was relatively low (we used a low coherence threshold and a phase window to select voxels for the target ROIs in the targets and flankers experiment), which could potentially reduce the spatial accuracy in defining ROIs on individual days. However, there are two reasons to believe that localization errors did not create the pattern of results we measured. First, the volume of the target ROIs was well-matched to the expected ROI sizes based on typical cortical magnification functions in human visual cortex, and the locations were repeatable, so we are confident that there were no gross errors in ROI definition. Secondly, the pattern of results in the superset ROIs was almost identical to the pattern of results in the target ROIs, even though the superset ROIs were roughly three times the volume of the target ROIs. The similarity of the responses in the small and large volumes of cortex indicates that the particular pattern of results we observed was not a consequence of sampling or spatial localization. It is clear therefore that the pattern of results we measured in the target and superset ROIs is a good characterization of the cortical BOLD response to the Gabor patches.

Like other studies investigating the spatial accuracy of the BOLD technique (Hulvershorn, Bloy, Leigh & Elliott, 2005; Kriegeskorte, Cusack et al. 2010; Olman,

Inati & Heeger, 2007), this study found that spatial accuracy is different in different regions of cortex: some of the sub-ROIs illustrated in Fig. 3 are reliably localized with precision better than 1 mm, while others show localization errors as large as several millimeters. Heterogeneity of spatial precision can be expected from both the geometry of the cortex and the geometry of the vasculature. Some target ROIs are near large veins (Subject 1, in particular, has one sub-ROI location near an obvious large vein in the calcarine sulcus), and their location can vary from experiment to experiment based on slight differences in the orientation of the subject's head in the scanner. Other target ROIs were simply on an outer surface of the cortex, rather than along a sulcus. Several of the sub-ROIs in Subject 2, the subject in which we found the lowest day-to-day repeatability in ROI location, were located on the posterior surface of the brain. Physiological noise and motion artifacts are more severe on the outer boundary of the cortex, where intensity changes in the image are abrupt and partial volume effects between gray matter and CSF make the voxels particularly sensitive to motion.

In spite of careful localization of target ROIs, we observed a strong response to the flanking Gabor patches (presented alone) in the target ROI, which suggests an inability to separate BOLD responses to visual features with centers separated by 1° of visual angle at 3° eccentricity (5 mm). It would be incorrect to attribute all of the spatial blurring of the signal to hemodynamic mechanisms. At least two additional sources of spatial blurring are present in the data. On the experimental side, the combined effects of subject motion and motion compensation, as well as the spatial registrations, cause blurring on a scale of a few millimeters. On the physiological side, neural activity is correlated over spatial scales much larger than a single neural column. Long-range horizontal connections in macaque monkeys can extend over a millimeter in either direction (Angelucci, Levitt, Walton, Hupe, Bullier & Lund, 2002; Grinvald, Lieke, Frostig & Hildesheim, 1994). Therefore, when investigating local contextual modulation,

it is reasonable to expect that responses to neighboring stimuli will be confounded by even high-resolution BOLD measurements.

Other studies finding a mismatch between BOLD and V1 neural responses

Ours is not the only recent study to find a pattern of BOLD results that is not fully explained by psychophysics or neurophysiology. In studying interactions between collinear bar stimuli (a central bar with a flanking bar on each side), Kinoshita, Gilbert and Das (2009) found that strong facilitation of the neural spike rate was accompanied by strong suppression in the optical imaging signal. This mismatch was measured only in the cortical area representing the central bar and not in the cortical area extending to include the flanking bars. The authors interpret this finding to suggest that the measured facilitation of spike rates is the result of complex interactions between excitatory and inhibitory inputs, which happen to result in a decreased hemodynamic response.

Another recent study has also reported an unexplained mismatch between the BOLD response to surround suppression and the estimated local neural response. Using center-surround stimuli and a range of stimulus sizes, Nurminen et al. (2009) measured perceptual summation and surround fields and found that they matched the size of neuronal summation and surround suppression reported in Cavanaugh, Bair, and Movshon (2002). The summation and surround field sizes measured with spin echo BOLD were, however, larger than the perceptual and neuronal summation fields. The measured response increased with increasing stimulus size in the psychophysics, fMRI, and model data until it reached the size of the summation field; the response then decreased until asymptoting near the size of the surround field except in the case of the fMRI data, in which the response continued decreasing for all stimulus sizes.

Explanations based on neurohemodynamic coupling

Because the neurophysiological underpinnings of the BOLD response are not fully understood, one set of explanations for the discrepancy between our BOLD data and the predictions from psychophysics are based on possible differences in neurohemodynamic coupling on a local scale or when strong inhibition is present. We measured the contrast response for single Gabor patches at 3° eccentricity, finding a monotonically increasing function for contrasts used in the target and flankers experiment (Fig. 6). This is consistent with many other studies that have found a linear relationship between the BOLD response and the underlying neural activity and verifies that the discrepancy we found between the BOLD response and predicted local neural activity is not simply a consequence of the small size of the stimuli or the relatively high resolution of the experiment.

One untested explanation is that the dominant local suppression resulting from parallel flankers might interrupt the neurohemodynamic coupling by blocking the neural population responding to the target stimulus from recruiting more blood flow as contrast increases. This would result in decreased BOLD signal as a result of increased oxygen consumption without concomitant increase in blood flow. While it has been shown in cerebellar cortex that activation of inhibitory neurons alone does not increase blood flow (Li & Iadecola, 1994; Mathiesen, Caesar, Akgören & Lauritzen, 1998; although see discussion of Pelled et al., 2009, below), it is not known how local blood flow responds to various combinations of excitatory and inhibitory neural activity.

As opposed to the potential under-recruitment of blood flow suggested above, a direct coupling between inhibitory neural activity and the hemodynamic response could also produce the result we observed. A recent paper by Pelled, et al. (2009) shows that the positive BOLD response in ipsilateral somatosensory cortex following denervation of one paw in a rat may be attributable to increased inhibitory interneuron activity in the absence of excitatory activity. If local inhibitory neural activity plays a key role in driving the BOLD response, then the decrease in BOLD response with increasing target

contrast could be explained by a reduction in the magnitude of inhibitory neural activity due to the reduction in local second-order contrast (Zenger-Landolt & Koch, 2001).

We have suggested two very different ways in which local neural computations with a strong inhibitory component could alter "normal" neurohemodynamic coupling. The energy demand of inhibitory neuronal activity and its subsequent effect on blood flow is unresolved (Attwell & Laughlin, 2001; Caesar, Thomsen & Lauritzen, 2003; Cauli et al., 2004; Patel, de Graaf, Mason, Rothman, Shulman & Behar, 2005; Vaucher, Tong, Cholet, Lantin & Hamel, 2000), and it may not be the case that arguments based on energetics are relevant because the energy demands of neural activity may not be directly related to the hemodynamic response (Devor, Hillman, Tian, Waeber, Teng, Ruvinskaya, Shalinsky, Zhu, Haslilnger, Narayanan, Ulbert, Dunn, Lo, Rosen, Dale, Kleinfield & Boas, 2008; Sotero & Trujillo-Barreto, 2007). Nonetheless a growing body of literature suggests that, as the balance between excitation and inhibition is shifted in a local neural population, the BOLD response is not easily predicted.

Explanations based on an insufficient model for the neural activity

The above arguments also point to a second type of explanation for the pattern of results we measure: the BOLD response reflects local neural computations (Logothetis, 2003) and cannot be predicted from a univariate metric such as the output of neurons tuned to the orientation of the target stimulus. Psychophysical techniques only estimate neural responses in one narrowly tuned neural population, while other local neural populations with different response properties also contribute to the BOLD response. For example, in our parallel flanker condition, second-order contrast (contrast between the target and flankers) decreases with increasing target contrast. A neural mechanism sensitive to this contrast (Larsson, Landy & Heeger, 2006), whether originating in V1 or modulating V1 by feedback, would have a decreased response with increasing target contrast. A mechanism like this could also become significant only on a local scale,

dominating only when the region of second-order contrast is large compared to the region of uniform contrast.

Similarly, the fact that adding a low-contrast target between orthogonal flankers decreased rather than increased the BOLD response (in both target and superset ROIs, Fig. 4D, 4E) might be explained by cross-orientation inhibition of neurons with receptive fields located so that they respond to both target and flanker Gabors. Given the complexity of neural responses in a single cubic millimeter of cortex, and the number of dimensions to which they are tuned, the models we use to predict V1 responses and interpret BOLD data are necessarily approximations – which may be valid in the case of extended sinusoidal gratings but fail for more localized stimuli.

A final possibility is that surround suppression might not originate in V1, and that we should not therefore expect the V1 BOLD response to match psychophysical measurements of suppression effects. Several researchers have suggested that feedback from higher visual areas is critical to contextual modulation (Zipser, Lamme et al. 1996; Hupe, James et al. 1998) and that the spatial scale of surround suppression is more consistent with the scale of feedback from higher visual areas than lateral connections within V1 (Angelucci, et al., 2002; Schwabe, Obermayer, Angelucci, & Bressloff, 2006). However, this would not explain why BOLD measurements of suppression are consistent with psychophysics for large patches of sinusoidal gratings but not for local measurements of individual Gabor patches. Further work is therefore required to understand the source of neural suppression in early visual cortex as well as to develop appropriate models of neural response properties that can predict the modulation of the high-resolution BOLD response by local image context.

An alternative to developing a complete model of local neural activity to explain the BOLD response is to analyze the pattern of results simply to ask whether it contains information about particular stimulus attributes. Many recent studies using multi-voxel patterned activity (MVPA) and decoding approaches (Kamitani & Tong, 2005; Kay,

Naselaris, Prenger & Gallant, 2008) have circumvented the problems of spatial resolution and neural complexity by taking an indirect approach to measuring patterned activity in visual cortex. Rather than insisting on a one-to-one match between a voxel's response and the underlying neural activity, MVPA and decoding approaches simply ask whether the patterned BOLD activity clearly distinguishes between different stimuli or brain states. While such analyses do not elucidate the underlying neural code, they are valuable for determining aspects of the stimulus to which a given brain area is sensitive. The experiment we report here suggests that such indirect approaches may be the best option for studying patterned activity with 3T GE BOLD, at least for distinguishing responses to stimuli whose neural representations lie within several millimeters of each other.

Summary

These experiments have shown (i) successful localization of a particular spatial location over days in subjects, (ii) an inability to separate BOLD responses to neighboring visual features separated by ~5 mm on cortex, and (iii) that, for the specific case of single Gabor patches flanked by parallel or orthogonal Gabors, high-resolution BOLD responses are not reliably correlated with V1 output predicted by psychophysical measurements. The response pattern we observed (decreasing BOLD response with increasing target contrast when flankers are parallel) could be explained by several factors, such as a strong effect of inhibitory interneurons in driving the BOLD response or a strong contribution from neurons other than the subset of the population that encode the target stimulus and serve the contrast discrimination task. Further work is necessary to determine how the neural model or the neurohemodynamic coupling model (or both) must be elaborated to treat sufficiently the case of local contextual modulation in primary visual cortex.

Chapter 4

Collinear Facilitation and Orientation-Dependent Inhibitory Mechanisms Operate on Different Spatial Scales in a Contour Detection Task

Authors: Jennifer F. Schumacher, Cheryl A. Olman

To be submitted to *Journal of Vision*

Abstract

Contour detection is a crucial component of visual processing; however performance on this task can vary depending on the arrangement or the context of the visual scene. Dakin and Baruch, 2009 showed that orientation of distracting elements affects detection of collinear elements, but there has not been a systematic study investigating both the configuration of the stimulus elements and contextual modulation. Using collinear Gabor elements in a field of distractor Gabor elements we measured the effects of eccentricity, spacing, and spatial frequency on contour detection performance in three different contexts: randomly oriented distractors (control condition), distractors aligned in parallel on either side of the collinear Gabors, and orthogonal distractors on either side of the collinear Gabors. In the control condition, we found that tolerance for orientation jitter improved when collinear Gabors were more widely spaced and larger in size. The parallel condition had a greater effect on threshold than the orthogonal condition for intermediate and large spacings and sizes while the orthogonal condition had a greater effect on threshold for the smallest spacing and size. The results show that collinear facilitation reduces with spacing and spatial frequency and orientation-dependent lateral masking releases suppression as spacing increases.

Introduction

Context, or the set of image features that surrounds the feature of interest, is an important factor that can either hinder or help one's performance in a visual task. In a contour detection task, Dakin and Baruch, 2009 found that collinear Gabor patches in a parallel context increased the detection threshold while an orthogonal context decreased the threshold. However, orientation-dependent contextual modulation is known to operate over a limited spatial scale, so the present work experiment explores the parameter space to see how orientation-dependent contextual modulation interactions with collinear facilitation.

Many studies have investigated contour integration and detection in primary visual cortex (V1). A mechanism thought to contribute to contour integration is collinear facilitation, where detection and contrast discrimination thresholds are decreased for collinear elements (Cass 2005; Cass, 2006; Polat, 1999; Kapadia, et al., 1995). Collinearity is critical for correct and quick contour detection and large degrees of "jitter", or the relative orientation of the individual elements to each other, greatly impedes contour detection (Nygard, et al., 2009; Field, et al., 1993). An anatomical basis supporting contour integration via collinear facilitation in V1 involves the long-range horizontal connections between similar orientation columns (Gilbert & Wiesel, 1989; Malach et al, 1993; Rockland et al, 1982; Schmidt et al, 1997; Bosking et al, 1997). However, it is unclear whether lateral connections are the sole mechanism behind contour integration or if feedback processes also contribute to this phenomenon. Contours often exist on scales larger than long-range horizontal connections; therefore it may be necessary to invoke mechanisms that operate over longer distances. While long-range connections can extend over about 2-4 mm (Angelucci, Levitt, Walton, Hupe, Bullier & Lund, 2002, Amir, Harel & Malach, 1993, Grinvald, Lieke, Frostig & Hildesheim, 1994; Blasdel, et al., 1985), local-global integration can occur on an even larger scale (6-9 mm) via feedback from higher visual areas ({Angelucci, et al., 2002, Hupe, et al., 1998; Zipser, et al., 1996).

It is also known that contour detection is dependent on the stimulus geometry and the spatial configuration of the visual scene (Bonneh & Sagi, 1998). Generally it has been found that with an increased spacing between Gabor elements, the performance in contour detection decreases (Kapadia, et al., 1995; Field, et al., 1993), however some distance is necessary for optimal collinear facilitation (2-3 lambda separation) ({Polat, 1999). Spatial frequency has shown little effect on contour integration, with good performance between 2 - 4.5 cycles per degree (cpd) (Dakin & Hess, 1998) and there are reports that contour integration is scale invariant (Hess & Dakin, 1997; Field, et al., 1993). Previous work on contour detection across eccentricity has found a decrease in performance in the far periphery (>10°), even after accounting for cortical magnification (Hess & Dakin, 1997; Shani & Sagi, 2005, Ito & Gilbert, 1999). The significant differences between foveal and peripheral performance when stimuli are presented at greater than 4° is most likely attributed to differences in spatial attention(Hess & Dakin, 1997; Field, et al., 1993; Shani & Sagi, 2005, Ito & Gilbert, 1999). However, there is no one study that systematically varies these three parameters for a single stimulus set and task, nor with analyzing the effect of contextual modulation over these parameters.

Contour detection within a field of randomly oriented distractors provides a baseline against which orientation-dependent surround effects can be measured. Orientation-dependent contextual modulation causes the response to a single or collinear Gabor elements to be enhanced with an orthogonal surround or suppressed with a parallel surround (Knierem & van Essen, 1992; Northdurft, et al., 1999; Solomon & Morgan, 2000; Zenger-Landolt & Koch, 2001; Dakin & Baruch, 2009). However, the levels of response enhancement and suppression in V1 are determined by the spatial frequency and stimulus contrast and as well as the spacing between the elements (Shani & Sagi, 2005; Angelucci & Bressloff, 2006; Dakin & Baruch, 2009). Our investigation of contour detection with orientation-dependent contextual modulation has revealed a significant effect from spacing and spatial frequency which suggests that contour detection is

optimal over a larger spatial scale and orientation-dependent effects are strongest at smaller spatial scales.

Methods and Materials

Subjects

Data were collected from seven subjects (four female, age 21 – 37, mean age 26.9) with normal or corrected to normal vision. The experimental protocols were approved by the Institutional Review Board at the University of Minnesota. Subjects provided written informed consent before participating in the experiments.

Stimuli

The stimuli consisted of a constant-size field of Gabor patches (total angular subtent: 11.7°) with a variable number of distractor elements as the spacing between the Gabors and spatial frequency of the Gabors changed. Each Gabor patch consisted of a sinusoidal grating modulated by a Gaussian envelope that varied with spatial frequency (2, 3.3, or 4 cpd; σ = 0.33/spatial frequency). Gabors were always presented at 80% contrast on a mean gray background. Phase was randomized, as previous work has shown phase polarity does not effect contour integration in the fovea or near periphery (Field, et al., 2000; Hess & Field, 1995; Hess & Field, 1999). A white square at the center of the field served as the fixation mark and provided feedback during the task by changing color (green or red). Stimuli were generated and presented with Matlab (Mathworks, Inc., Natick, MA) and Psychtoolbox (Brainard, 1997; Pelli, 1997) and an iMac computer with OS X served as the processor. Stimuli were displayed on a NEC 2180UX LCD monitor, subtending 18.7 x 24.5 degrees of visual angle at a viewing distance of 100 cm.

Psychophysics

During each trial, one side of the Gabor element field contained five elements ("collinear Gabors") that were aligned with one of six levels of orientation jitter. The collinearity of these Gabors varied, at six levels from 0 to $\pi/4$ radians. The eccentricity at which the collinear Gabors were presented, the spacing between the Gabor elements, and the spatial frequency of the Gabor patches varied per block (each block contained 25 trials per jitter level per context, for a total of 450 trials presented in random order per block). Tolerance to orientation jitter was then measured using the method of constant stimuli. Parameters for each stimulus configuration varied as follows: 7 eccentricites (1.2°, 1.6°, 1.8°, 2.4°, 3°, 3.2°, 3.6°), 3 spacings (0.6°, 0.8°, 1.2°), and 3 spatial frequencies (2 cycles per degree (cpd), 3.3 cpd, 4 cpd). Eighteen specific configurations from this parameter space were used. The contextual environments included a control condition, where the orientation of the elements on either side of the vertical line of Gabors forming the target contour was random, a "parallel" condition where the orientation of the surround elements was drawn from a distribution of orientations parallel to the target Gabors (uniformly distributed, [pi/4 3pi/4], where 0 is vertical), and an "orthogonal" condition where the orientation of the surround elements was drawn from a distribution of orientations orthogonal to the target Gabors (uniformly distributed, [pi/4 3pi/4]). Distractor elements were drawn from a uniform distribution [0 pi], but relative orientation of neighboring distracters was controlled to avoid collinearities ($\Delta\theta >$ pi/6). The two flanking lines were present on both sides of the visual field on every trial. Three stimulus exemplars are shown in Figure 4.1.

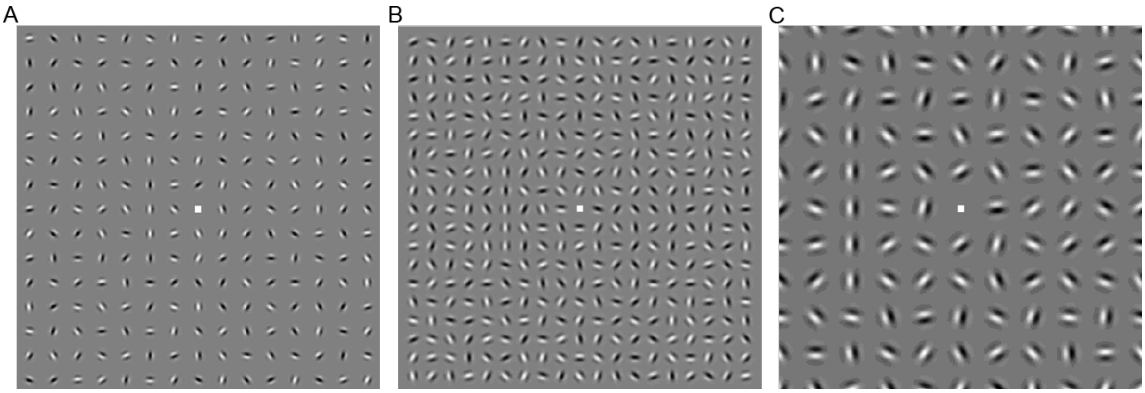

Figure 4.1: Examples of stimuli with collinear Gabors present on the left side. A) Control condition (randomly oriented flanking distracters) : in this example, the target contour was presented at 1.6° eccentricity, with both the collinear and distractor Gabors presented with 0.8° spacing and 4 cpd spatial frequency. B) Parallel condition: in this example, the target contour was presented at 2.4° eccentricity, with both the collinear and distractor Gabors presented with 0.6° spacing and 3.3 cpd spatial frequency. The orientations of the distractor Gabors were drawn from a distribution of orientations parallel to the collinear Gabors. C) Orthogonal condition: in this example, the target contour was presented at 3.6° eccentricity, with both collinear and distractor Gabors presented with 1.2° spacing and 2 cpd spatial frequency. The orientation of the distractor Gabors were drawn from a distribution of orientations orthogonal to the collinear Gabors.

In a two alternative forced choice (2AFC) paradigm, subjects responded left or right to indicate where the (jittered) contour appeared. The stimulus was presented for 150 ms on each trial with unlimited time for subjects to respond and a 500 ms pause after the response and before the onset of the next trial. Subjects maintained fixation on the fixation square at the center of the screen; feedback was given by the fixation mark turning green for a correct response and red for an incorrect response, and disappeared in between trials. Psychometric functions for each stimulus configuration and context (54 total conditions) were estimated from each subject's performance.

Analysis

Psychometric functions were fit with the Psignifit toolbox (Psignifit) with Matlab.Performance over six levels of jitter (orientation of the collinear Gabors) was fit with a Weibull function using maximum-likelihood estimation and 2000 iterations of bootstrapping (Figure 4.2). Thresholds were taken from the 75% correct fit point. One

subject's thresholds were significantly lower than the other six subjects, so this subject was excluded from further analysis. Thresholds were then averaged over the remaining six subjects per stimulus type and condition. Normalized thresholds, or suppression indices, for the parallel and control conditions were obtained by subtracting the parallel or control threshold from the orthogonal threshold per subject, then averaging.

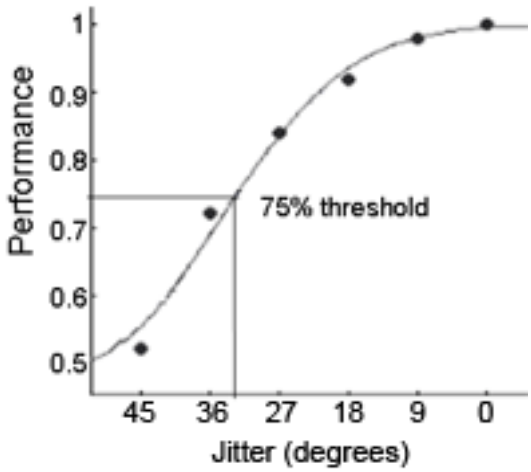

Figure 4.2: Example of a psychometric function (control context, 1.2° eccentricity, 0.6° spacing, 3.3 cpd, subject 1). Percent correct is plotted for six levels of jitter ,along with the Weibull function fit to data using maximum-likelihood estimation (2000 bootstrapping iterations) using the Psignifit toolbox with Matlab.

Results

We measured human subjects' performance for contour detection in three contexts (control, parallel, and orthogonal – referring to the orientation of the distractor Gabor elements immediately adjacent to the target contour) at eighteen different stimulus configurations differing in eccentricity, spacing, and spatial frequency. Performance thresholds were used to evaluate the interaction of the parameter space and context versus the subjects' performance in a collinear detection task.

Performance for the control condition is plotted in Figure 4.3. Comparisons of interest in the parameter space are described in Figure 4.3A. Across eccentricity (Figure 4.3B), performance generally decreased, but there performance was better with elements

that were further apart (dashed line versus solid line). In keeping with previous literature, performance was worst for the smallest spacing (0.6° or 2λ), increased for an optimal spacing (0.8° or 2.7 λ) and decreased again for a larger spacing (1.2° or 4λ) (Figure 4.3C) (Polat, 1999). A similar, but weaker trend is seen across spatial frequency (Figure 4.3D, 1.6 λ – 3.2 λ), consistent with Dakin & Hess (1998).In contradiction to previous reports, contour detection was not scale invariant: performance increased significantly as the elements were spaced further apart and larger in size (Figure 4.3E, p = 0.0008, ANOVA). The increase in performance when spacing and spatial frequency also scaled with eccentricity (Figure 4.3F, p = 0.0149, 2-way ANOVA).

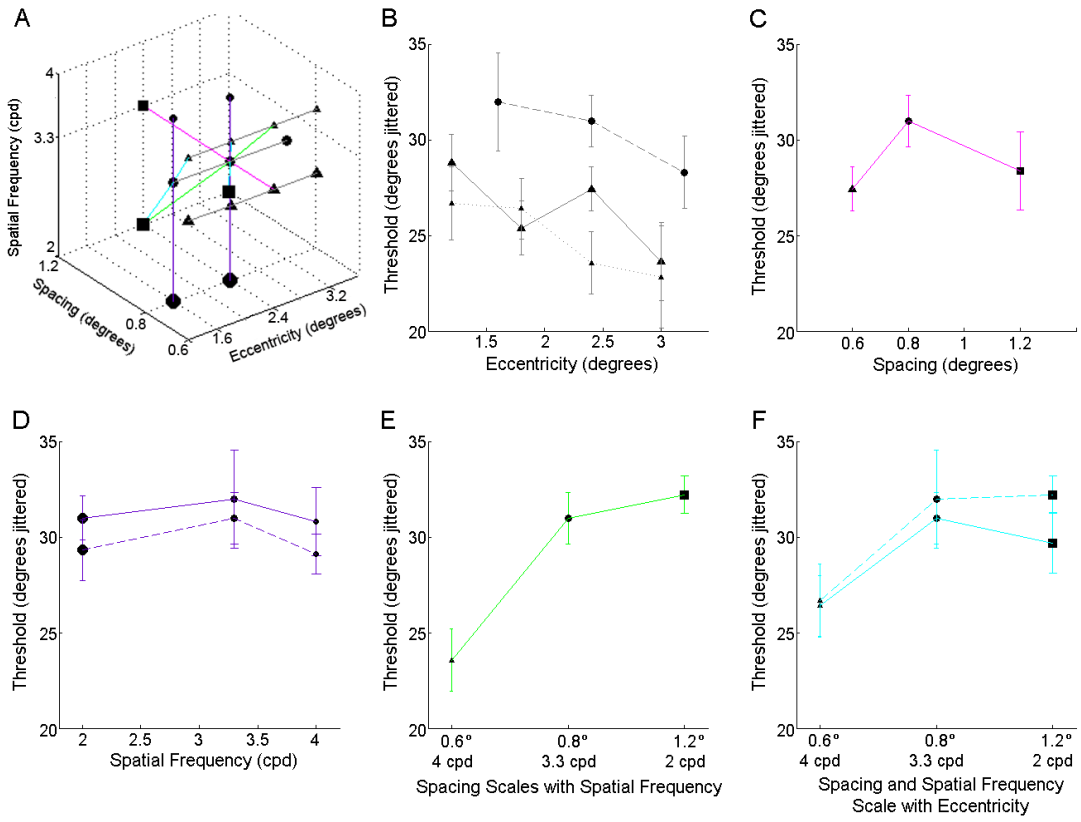

Figure 4.3: Control condition results. A) Representation of parameter space. Color-coded lines indicate comparisons shown in panels B-F. Marker shapes indicate spacing (0.6°: triangle, 0.8°: circle, and 1.2°: square); marker size indicates spatial frequency (larger markers for lower spatial

frequencies). B) Dependence of performance on eccentricity. Solid line is 0.6° spacing and 3.3 cpd, dashed line is 0.8° spacing and 3.3 cpd, dotted line is 0.6° spacing and 4 cpd. C) Performance as a function of spacing for 3.3 cpd Gabors at 2.4 ° eccentricity. D) Performance as a function of element size, for elements spaced at 0.8° with target contours at 1.6° eccentricity (solid line) and 2.4° eccentricity (dashed line). E) Performance increased as the elements were spaced further apart and larger in size was statistically significant, p = 0.001), even though the relative spacing (spacing/) was almost constant (2.4λ-2.7λ). Eccentricity was 2.4°. F) Performance improved as elements were moved toward the periphery and scaled according to cortical magnification (p = 0.015). The solid line covered eccentricities 1.2°, 1.6°, and 2.4°, the dashed line covered eccentricities 1.8°, 2.4°, and 3.6°. Error bars for plots B-F are SEM, n = 6.

Consistent with previous reports, collinear facilitation is scale invariant when the target contour is flanked by orthogonal distractors as performance is relatively consistent across eccentricity (Figure 4.4B). Performance decreased with either an increase in spacing or an increase in spatial frequency (Figure 4.4C-D). Both of these changes increase the relative spacing of the elements (covering a range from 1.2λ to 4λ), so this pattern is in keeping with previous literature reports. The decrease in performance is significant in the case of spatial frequency (p = 0.03, 2-way ANOVA). However, similar to the control condition, there is an increase in performance as the elements were place further apart and larger at a fixed eccentricity (Figure 4.4E).

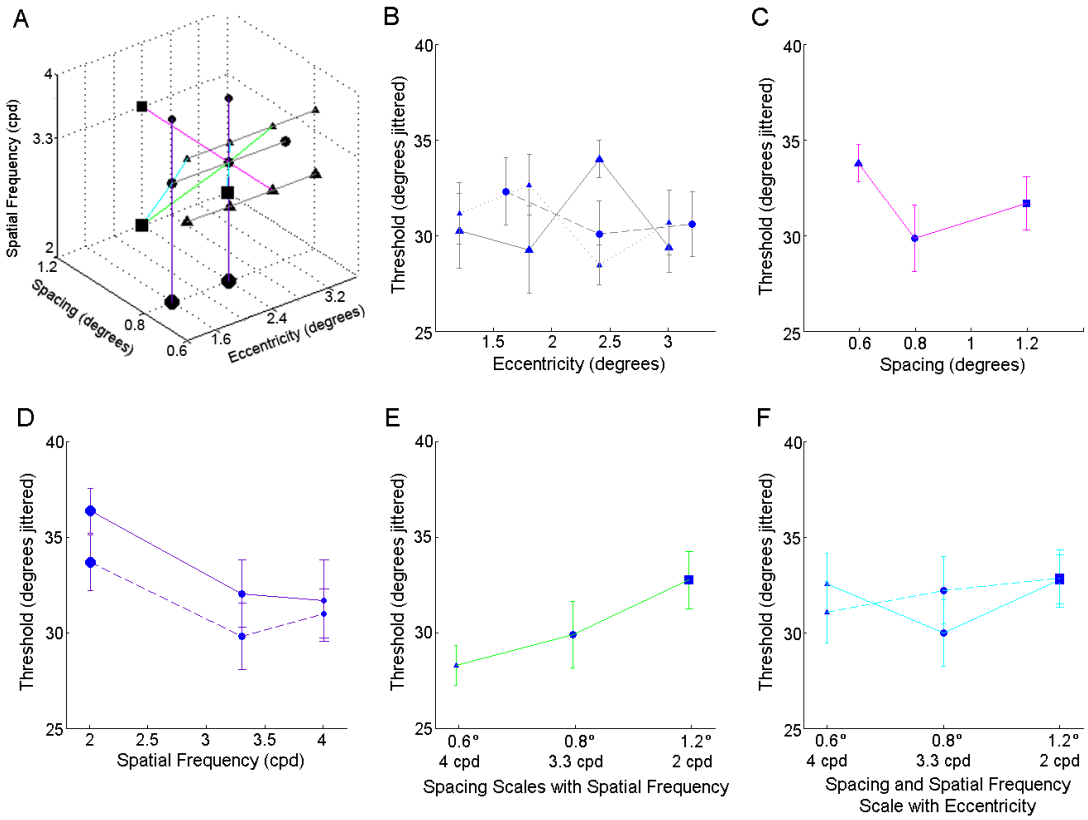

Figure 4.4: Orthogonal context results - collinear facilitation dominates. Data are plotted as in Figure 4.3. D) The decrease in performance over spatial frequency was statistically significant, p = 0.03, 2-way ANOVA.

Finally, to view the effects of orientation-dependent lateral masking, the control and parallel conditions were subtracted from the orthogonal condition (Figure 4.5). The greatest effect of lateral masking is seen as a function of spacing and spatial frequency, where increasing either of these parameters brought performance back to the level of the orthogonal condition (Figure 4.5C-D, control condition was significant in both cases: spacing: p =0.05, ANOVA; spatial frequency: p = 0.01, 2-way ANOVA). This pattern is consistent with a model in which contour detection performance is determined by a balance between collinear facilitation, which weakens with increasing spacing or decreasing size, and orientation-dependent lateral masking, which is strongest for parallel

or large distractors and decreases with spacing. Correspondingly, suppression from lateral masking decreased as elements were placed further apart and larger for the control condition but was consistently strong in the parallel condition (Figure 4.5E). Finally, both conditions increased in performance (or at least maintained performance relative to the orthogonal condition, parallel condition, dashed line) as elements were placed further in the periphery, spaced further apart, and larger in size compared to elements closer to the fovea, spaced close together, and smaller in size (Figure 4.5F).

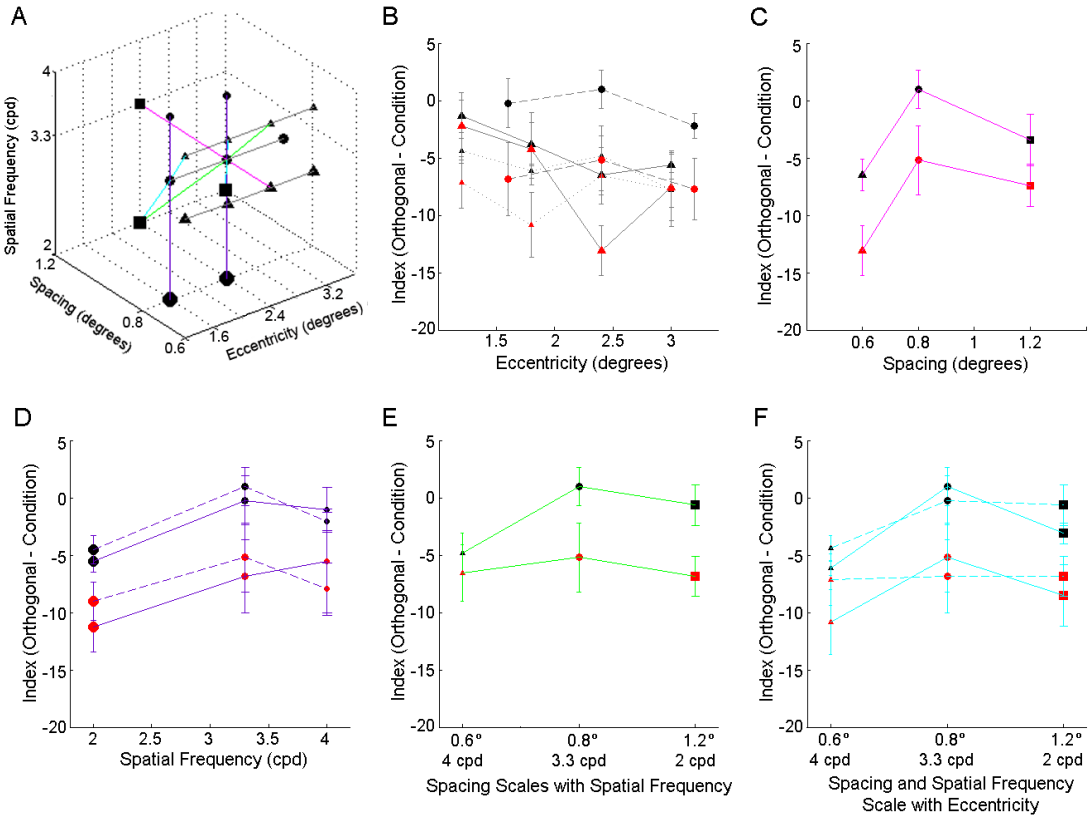

Figure 4.5: Performance on control and parallel condition relative to orthogonal condition. Indices were calculated by subtracting thresholds from the control or parallel conditions from the thresholds of the orthogonal condition. Black markers represents the control condition and red markers indicate the parallel condition. Data plotted as in Figure 4.3. C) The control condition was statistically significant, p = 0.05, ANOVA. D) The trend of the control condition was statistically significant p = 0.01, 2-way ANOVA. F) Both conditions were statistically significant, across scaling for the control condition, p = 0.005, 2-way ANOVA and across the different eccentricities covered for the parallel condition, p = 0.04, 2-way ANOVA.

Discussion

We have expanded upon Dakin and Baruch, 2009 to establish some guiding principles for the effect of lateral masking on contour integration. We have confirmed the optimal ranges of collinear facilitation: 2-3λ for spacing and 2-4.5 cpd for spatial frequency (Polat, 1999; Dakin & Hess, 1998). However, our results also show there is a balance of collinear facilitation with lateral masking as spacing and spatial frequency interacts, when elements are within 4λ of each other, and orientation-dependent lateral masking has a strong effect on contour detection performance.

Lateral masking, a mechanism which induces suppression due to overlapping cortical representations, likely contributes to the decrease in performance when elements were closely spaced. Here we found the greatest lateral masking for 0.6° and 3.3 cpd (2λ) and 0.8° and 2 cpd (1.6λ) in the control and parallel conditions. Thus, lateral masking operates over limited cortical spaces. The cortical scale limitations of lateral masking also likely explain why performance increased significantly as the elements were spaced further apart and larger in size. This pattern of results is consistent with model predictions on contour integration and saliency by Mundhenk and Itti, 2005.

The visual spatial range of collinear facilitation (slightly larger) and lateral masking (slightly smaller) also coordinates with cortical representations. For example, using human cortical magnification estimates (Engel, et al., 1997) at 2.4° eccentricity, the smallest spacing (0.6°) extends about 3.5 mm, intermediate spacing (0.8°) extends about 4.6 mm, and largest spacing (1.2°) extends about 6.4 mm. Lateral masking supports a short-range neural mechanism (such as long-range horizontal connections in V1 extending ~3 mm (Angelucci, Levitt, Walton, Hupe, Bullier & Lund, 2002, Amir, Harel & Malach, 1993, Grinvald, Lieke, Frostig & Hildesheim, 1994; Blasdel, et al., 1985)) while the collinear facilitation supports a long-range neural mechanism (such as feedback

or global pooling over an area greater than 6 mm) (Angelucci, et al., 2002, Hupe, et al., 1998; Zipser, et al., 1996).

Lateral masking is also orientation-dependent. This mechanism is minimal in the orthogonal condition, where collinear facilitation dominates, and serves as a baseline to compare the amount of suppression with the orientation of the distractors (Figure 4.5). As the orientation of the distractors moves closer to the orientation of the target contour, contour detection performance is reduced (control and parallel conditions). This effect was dependent on the spacing and spatial frequency of the elements, decreasing both with increased separation between the cortical representations of individual elements and with decreased size. There was also a dependence on eccentricity, where lateral masking further suppressed performance as the contour was placed further in the periphery – consistent again with a lateral masking mechanism that scales with distance on the cortical surface.

Conclusion

Contour detection and orientation-dependent lateral masking operate on different spatial scales. Collinear facilitation and lateral masking both fall off with increasing distance, but lateral masking falls off faster, making it consistent with the length of long-range horizontal connections in V1 while collinear facilitation acts over longer distances. Both mechanisms are tuned to orientation, where lateral masking was strongest when the distractor elements were aligned randomly or parallel to the collinear elements and this orientation dependence also changed with spacing and spatial frequency.

Bibliography

Ackermann, R.F., Finch, D.M., & Babb, T.L. (1984). Increased glucose metabolism during long-duration recurent inhibition of hippocampal pyramidal cells. *Journal of Neuroscience, 4* (1), 251-264.

Adriany, G., J. Pfeuffer, et al. (2001). *A half-volume transmit/receive coil combination for 7 Tesla applications.* 9th Annual Scientific Meeting of the ISMRM, Glasgow.

Amir, Y., M. Harel, et al. (1993). Cortical hierarchy reflected in the organization of intrinsic connections in macaque monkey visual cortex. *Journal of Comparative Neurology* **334**(1): 19-46.

Angelucci, A., J. B. Levitt, et al. (2002). Circuits for local and global signal integration in primary visual cortex. *Journal of Neuroscience* **22**(19): 8633-8646.

Bandettini, P. A., A. Jesmanowicz, et al. (1993). Processing strategies for time-course data sets in functional MRI of the human brain." Magnetic Resonance in Medicine **30**(2): 161-173.

Bandettini, P. A., E. C. Wong, et al. (1994). Spin-echo and gradient-echo EPI of human brain activation using BOLD contrast: a comparative study at 1.5 T. *NMR in Biomedicine* **7**(1-2): 12-20.

Blasdel, G. G., J. S. Lund, et al. (1985). "Intrinsic connections of macaque striate cortex: axonal projections of cells outside lamina 4C." *Journal of Neuroscience* **5**(12): 3350-69.

Bonneh, Y. and D. Sagi (1998). "Effects of spatial configuration on contrast detection." *Vision Research* **38**(22): 3541-53.

Bosking, W.H., Zhang, Y., Schofield, B., Fitzpatrick, D. (1997). Orientation selectivity and the arrangement of horizontal connections in tree shrew striate cortex. *Journal of Neuroscience* **17**(6): 2112-2127.

Boynton, G. M., J. B. Demb, et al. (1999). Neuronal basis of contrast discrimination. *Vision Research* **39**: 257-269.

Boynton, G. M., S. A. Engel, et al. (1996). Linear systems analysis of functional magnetic resonance imaging in human V1. *Journal of Neuroscience* **16**(13): 4207-4221.

Brainard, D.H. (1997). The psychophysics toolbox. *Spatial Vision, 10,* 433-436.

Buracas, G. T. and G. M. Boynton (2007). The effect of spatial attention on contrast response functions in human visual cortex. *Journal of Neuroscience* **27**(1): 93-97.

Caesar, K., Thomsen, K., & Lauritzen, M. (2003). Dissociation of spikes, synaptic activity, and activity-dependent increments in rat cerebellar blood flow by tonic synaptic inhibition. *Proceedings of the National Academy of Sciences, USA, 100* (26), 16000 -16005.

Cass, J.R. & Spehar, B. (2005). Dynamics of collinear contrast facilitation are consistent with long-range horizontal striate transmission. *Vision Research,* 45, 2728-2739.

Cass, J. & Alais, D. (2006). The mechanisms of collinear integration. *Journal of Vision*, 6, 915-922.

Cauli, B., Tong, X.K., Rancillac, A., Serluca, N., Lambolez, B., Rossier, J., & Hamel, E. (2004). Cortical GABA interneurons in neurovascular coupling: relays for subcortical vasoactive pathways. *Journal of Neuroscience, 24* (41), 8940-8949.

Cavanaugh, J.R., Bair, W., & Movshon, J.A. (2002). Selectivity and spatial distribution of signals from the receptive field surround of macaque V1 neurons. *Journal of Neurophysiology, 88*, 2547-2556.

Chen, Z., Silva, A.C., Yang, J., & Shen, J. (2005). Elevated endogenous GABA level correlates with decreased fMRI signals in the rat brain during acute inhibition of GABA transaminase. *Journal of Neuroscience Research, 79*, 383-391.

Cheng, K., R. A. Wagooner, et al. (2001). Human ocular dominance columns as revealed by high-field functional magnetic resonance imaging. *Neuron* **32**: 359-374.

Crist, R. E., W. Li, et al. (2001). Learning to see: experience and attention in primary visual cortex." *Nature Neuroscience* **4**(5): 519-525.

Dakin, S. C. and N. J. Baruch (2009). "Context influences contour integration." *Journal of Vision* **9**(2): 13 1-13.

Dakin, S. C. and R. F. Hess (1998). "Spatial-frequency tuning of visual contour integration." *J Opt Soc Am A Opt Image Sci Vis* **15**(6): 1486-99.

Das, A., & Gilbert, C.D. (1995). Long-range horizontal connections and their role in cortical reorganization revealed by optical recording of cat primary visual cortex. *Nature, 375*, 780-784.

Devor, A., Hillman, E.M.C., Tian, P., Waeber, C., Teng, I.C., Ruvinskaya, L., Shalinsky, M.H., Zhu, H., Haslilnger, R.H., Narayanan, S.N., Ulbert, I., Dunn, A.K., Lo, E.H., Rosen, B.R., Dale, A.M., Kleinfield, D., & Boas, D.A. (2008). Sitmulus-induced changes in blood flow and 2-deoxyglucose uptake dissociate in ipsilateral somatosensory cortex. *Journal of Neuroscience, 28* (53), 14347-14357.

Devor, A., Tian, P., Nishimura, N., Teng, I.C., Hillman, E.M.C., Narayanan, S.N., Ulbert, I., Boas, D.A., & Kleinfield, D. (2007). Suppressed neuronal activity and concurrent arteriolar vasoconstriction may explain negative blood oxygenation level-dependent signal. *Journal of Neuroscience, 27* (16), 4452-4459.

DeYoe, E. A., G. J. Carman, et al. (1996). Mapping striate and extrastriate visual areas in human cerebral cortex. *Proceedings of the National Academy of Sciences, USA* **93**: 2382-2386.

Duong, T. Q., D.-S. Kim, et al. (2001). Localized cerebral blood flow response at sub-millimeter columnar resolution. *Proceedings of the National Academy of Sciences, USA* **95**: 11489-11492.

Duong, T. Q., E. Yacoub, et al. (2003). Microvascular BOLD contribution at 4 and 7 T in the human brain: gradient-echo and spin-echo fMRI with suppression of blood effects. *Magnetic Resonance in Medicine* **49**: 1019-1027.

Engel, S. A., G. H. Glover, et al. (1997). Retinotopic organization in human visual cortex and the spatial precision of functional MRI. *Cerebral Cortex* **7**: 181-192.

Field, D.J., Hayes, A., Hess, R.F. (1993). Contour integration by the human visual system: evidence for a local "association field." *Vision Research* **33**(2): 173-193.

Gilbert, C.D. & Wiesel, T.N. (1989). Columnar specificity of intrinsic horizontal and corticocortical connections in cat visual cortex. *Journal of Neuroscience*, 9, 2432-2442.

Grigorescu, C., N. Petkov, et al. (2004). Contour and boundary detection improved by surround suppression of texture edges. *Image and Vision Computing* **22**: 609-622.

Grinvald, A., E. E. Lieke, et al. (1994). Cortical point-spread function and long-range lateral interactions revealed by real-time optical imaging of macaque monkey primary visual cortex. *Journal of Neuroscience* **14**(5): 2545-2568.

Grossberg, S., & Williamson, J.R. (2001). A neural model of how horizontal and interlaminar connections of visual cortex develop into adult circuits that carry out perceptual grouping and learning. *Cerebral Cortex, 11* (1), 37-58.

Hecht, S., S. Shlaer, et al. (1942). Energy, Quanta, and Vision. *Journal of General Physiology* **25**(6): 819-840.

Heckman, G. M., S. E. Bouvier, et al. (2007). Nonlinearities in rapid event-related fMRI explained by stimulus scaling. *NeuroImage* **34**: 651-660.

Hess, R. and D. Field (1999). Integration of contours: new insights. *Trends Cognitive Science* **3**(12): 480-486.

Hess, R. F. and S. C. Dakin (1997). Absence of contour linking in peripheral vision. *Nature* **390**(6660): 602-4.

Hess, R. F. and D. J. Field (1995). Contour integration across depth. *Vision Research* **35**(12): 1699-711.

Hulvershorn, J., L. Bloy, et al. (2005). Spatial sensitivity and temporal response of spin echo and gradient echo bold contrast at 3T using peak hemodynamic activation time. *NeuroImage* **24**: 216-223.

Hupe, J. M., A. C. James, et al. (1998). Cortical feedback improves discrimination between figure and background by V1, V2 and V3 neurons. *Nature* **394**(6695): 784-7.

Ito, M. and C. D. Gilbert (1999). Attention modulates contextual influences in the primary visual cortex of alert monkeys. *Neuron* **22**(3): 593-604.

Jenkinson, M., Bannister, P.R., Brady, J.M., Smith, S.M. (2002) Improved optimization for the robust and accurate linear registration and motion correction of brain images. *NeuroImage,* **17**(2), 825-841.

Kamitani, Y. and F. Tong (2005). "Decoding the visual and subjective contents of the human brain." *Nature Neuroscience* **8**(5): 679-685.

Kapadia, M.K., Ito, M., Gilbert, C.D. Westheimer, G. (1995). Improvement of visual sensitivity by changes in local context: parallel studies in human observers and in V1 of alert monkeys. *Neuron*, 4: 843-856.

Kastner, S., De Weerd, P., Pinsk, M.A., Elizondo, M.I., Desimone, R., & Ungerleider, L.G. (2001). Modulation of sensory suppression: implications for receptive field sizes in the human visual cortex. *Journal of Neurophysiology, 86*, 1398-1411.

Kay, K. N., T. Naselaris, et al. (2008). Identifying natural images from human brain activity." *Nature* **452**: 352-355.

Kinoshita, M., Gilbert, C.D., & Das, A. (2009). Optical imaging of contextual interactions in V1 of the behaving monkey. *Journal of Neurophysiology, 102*, 1930-1944.

Knierim, J. J. and D. C. van Essen (1992). Neuronal responses to static texture patterns in area V1 of the alert macaque monkey. *Journal of Neurophysiology* **67**(4): 961-80.

Kriegeskorte, N., R. Cusack, et al. (2009). How does an fMRI voxel sample the neuronal activity pattern: Compact-kernel or complex spatiotemporal filter? *Neuroimage.*

Larsson, J. (2001). Imaging vision: functional mapping of intermediate visual processes in man. Stockholm, Sweden, Karolinska Institutet.

Li, J., & Iadecola, C. (1994). Nitric oxide and adenosine mediate vasodilation during functional activation in cerebellar cortex. *Neuropharmacology, **33*** (11), 1453-1461.

Logothetis, N. K., J. Pauls, et al. (2001). Neurophysiological investigation of the basis of the fMRI signal. *Nature* **412**(6843): 150-157.

Logothetis, N.K. (2003). The underpinnings of the BOLD functional magnetic resonance imaging signal. *Journal of Neuroscience,* **23** (10), 3963-3971.

Maier, A., M. Wilke, et al. (2008). Divergence of fMRI and neural signals in V1 during perceptual suppression in the awake monkey. *Nature Neuroscience* **11**(10): 1193.

Malach, R., Harel, A.M., Grinvald, A. (1993). Relationship between intrinsic connections and functional architecture revealed by optical imaging and in vivo targeted biocytin injections in primate striate cortex. *Proceedings of the National Academy of Sciences, USA*, 90: 10469-10473.

Mathiesen, C., Caesar, K., Akgören, N., & Lauritzen, M. (1998). Modification of activity-dependent increases of cerebral blood flow by excitatory synaptic activity and spikes in rat cerebellar cortex. *Journal of Physiology, 512* (2), 555-566.

Nestares, O. and D. J. Heeger (2000). "Robust multiresolution alignment of MRI brain volumes." *Magnetic Resonance in Medicine* **43**: 705-715.

Nie, F., & Wong-Riley, M.T.T. (1995). Double labeling of GABA and cytochrome oxidase in the macaque visual cortex: quantitative EM analysis. *Journal of Comparative Neurology, 356*, 115-131.

Norris, D. G., S. Zysset, et al. (2002). An investigation of the value of spin-echo-based fMRI using a Stroop color-word matching task and EPI at 3 T. *NeuroImage* **15**(3): 719-726.

Nothdurft, H. C., J. L. Gallant, et al. (1999). Response modulation by texture surround in primate area V1: correlates of "popout" under anesthesia. *Vis Neurosci* **16**(1): 15-34.

Northoff, G., Walter, M., Schulte, R.F., Beck, J., Dydak, U., Henning, A., Boeker, H., Grimm, S., & Boesiger, P. (2007). GABA concentrations in the human anterior cingulate cortex predict negative BOLD responses in fMRI. *Nature Neuroscience, 10*, 1515-1517.

Nurminen, L., Kilpeläinen, M., Laurinen, P., Vanni, S. (2009) Area summation in human visual system: psychophysics, fMRI and modeling. *Journal of Neurophysiology*, article in press.

Nygard, G. E., T. V. Looy, et al. (2009). The influence of orientation jitter and motion on contour saliency and object identification. *Vision Research* **49**(20): 2475-84.

Ogawa, S., R. S. Menon, et al. (1993). Functional brain mapping by blood oxygenation level-dependent contrast magnetic resonance imaging: A comparison of signal characteristics with a biophysical model. *Biophysical Journal* **64**(3): 803-912.

Oja, J. M. E., J. Gillen, et al. (1999). Venous blood effects in spin-echo fMRI of human brain. *Magnetic Resonance in Medicine* **42**(4): 617-626.

Olman, C.A., Inati, S., & Heeger, D.J. (2007). The effect of large veins on spatial localization with GE BOLD at 3T: Displacement, not blurring. *NeuroImage, 34*, 1126-1135.

Parkes, L. M., J. V. Schwarzbach, et al. (2005). Quantifying the spatial resolution of the gradient echo and spin echo BOLD response at 3 Tesla. *Magnetic Resonance in Medicine* **54**: 1465-1472.

Patel, A. B., R. A. de Graaf, et al. (2005). The contribution of GABA to glutamate/glutamine cycling and energy metabolism in the rat cortex in vivo. *Proceedings of the National Academy of Sciences, USA* **102**(15): 5588-5593.

Pelled, G., D. A. Bergstrom, et al. (2009). Ipsilateral cortical fMRI responses after peripheral nerve damage in rats reflect increased interneuron activity. *Proceedings of the National Academy of Sciences, USA* **106**(33): 14114-9.

Pelli, D.G. (1997). The VideoToolbox software for visual psychophysics: transforming numbers into movies. *Spatial Vision,* 10, 437-442.

Petrov, Y., Carandini, M., & McKee, S. (2005). Two distinct mechanisms of suppression in human vision. *Journal of Neuroscience, 25* (38), 8704-8707.

Pihlaja, M., Henriksson, L., James, A.C., & Vanni, S. (2008). Quantitative multifocal fMRI shows active suppression in human V1. *Human Brain Mapping, 29,* 1001-1014.

Polat, U., Mizobe, K., Pettet, M.W., Kasamatsu, T., & Norcia, A.M. (1998). Collinear stimuli regulate visual responses depending on cell's contrast threshold. *Nature, 391*, 580-584.

Polat, U. (1999). Functional architecture of long-range perceptual interactions. *Spatial Vision***, 12**(2): 143-62.

Polat, U. & Bonneh, Y. (1999). Collinear interactions and contour integration. *Spatial Vision*, **13**(4), 393-401.

Ress, D. and D. J. Heeger (2003). Neuronal correlates of perception in early visual cortex. *Nature Neuroscience* **5**(4): 414-420.

Rockland, K.S. and Lund, J.S. (1982). Widespread periodic intrinsic connections in the tree shrew visual cortex. *Science,* 215(4539): 1532-1534.

Schwabe, L., Obermayer, K., Angelucci, A., & Bressloff, P.C. (2006). The role of feedback in shaping the extra-classical receptive field of cortical neurons: a recurrent network model. *Journal of Neuroscience,* 26 (36), 9117-9129.

Sereno, M. I., A. M. Dale, et al. (1995). Borders of multiple visual areas in humans revealed by functional magnetic resonance imaging. *Science* **268**(5212): 889-893.

Shani, R. and D. Sagi (2005). Eccentricity effects on lateral interactions. *Vision Research* **45**(15): 2009-24.

Shmuel, A., M. Augath, et al. (2006). "Negative functional MRI response correlates with decreases in neuronal activity in monkey visual area V1." *Nature Neuroscience* **9**(4): 569-577.

Smith, S. M., M. Jenkinson, et al. (2004). Advances in functional and structural MR image analysis and implementation as FSL. *NeuroImage* **23**(S1): 208-219.

Solomon, J. A. and M. J. Morgan (2000). Facilitation from collinear flanks is cancelled by non-collinear flanks. *Vision Research* **40**(3): 279-86.

Sotero, R.C., & Trujillo-Barreto, N.J. (2007). Modelling the role of excitatory and inhibitory neuronal activity in the generation of the BOLD signal. *NeuroImage, 35,* 149-165.

Stefanovic, B., J. M. Warnking, et al. (2004). Hemodynamic and metabolic responses to neuronal inhibition. *Neuroimage* **22**(2): 771-8.

Tolias, A.S., Sultan, F., Augath, M., Oeltermann, A., Tehovnik, E.J., Schiller, P.H., & Logothetis, N.K. (2005). Mapping cortical activity elicited with electrical microstimulation using fMRI in the macaque. *Neuron, 48,* 901-911.

Vaucher, E., Tong, X.-K., Cholet, N., Lantin, S., & Hamel, E. (2000). GABA neurons provide a rich input to microvessels but not nitric oxide neurons in the rat cerebral cortex: a means for direct regulation of local cerebral blood flow. *The Journal of Comparative Neurology, 421,* 161-171.

Wichmann, F. A. and N. J. Hill (2001). The psychometric function: I. Fitting, sampling, and goodness of fit. *Percept Psychophys* **63**(8): 1293-313.

Williams, A.L., Singh, K.D., & Smith, A.T. (2003). Surround modulation measure with functional MRI in the human visual cortex. *Journal of Neurophysiology, 89,* 525-533.

Xing, J., & Heeger, D.J. (2000). Center-surround interactions in foveal and peripheral vision. *Vision Research, 40,* 3065-3072.

Yacoub, E., T. Q. Duong, et al. (2003). Spin-echo fMRI in humans using high spatial resolutions and high magnetic fields. *Magnetic Resonance in Medicine* **49**: 655-664.

Yacoub, E., N. Harel, et al. (2008). High-field fMRI unveils orientation columns in humans. *Proceedings of the National Academy of Sciences, USA* **105**(30): 10607-10612.

Yacoub, E., A. Shmuel, et al. (2007). Robust detection of ocular dominance columns in humans using Hahn Spin Echo BOLD functional MRI at 7 Tesla. *NeuroImage* **37**(4): 1161-1177.

Zenger-Landolt, B. and C. Koch (2001). Flanker effects in peripheral contrast discrimination - psychophysics and modeling. *Vision Research* **41**: 3663-3675.

Zhang, N., X.-H. Zhu, et al. (2008). Investigating the source of BOLD nonlinearity in human visual cortex in response to paired visual stimuli. *NeuroIma*ge **43**(2): 204-212.

Zipser, K., V. A. Lamme, et al. (1996). Contextual modulation in primary visual cortex. *Journal of Neuroscience* **16**(22): 7376-89.